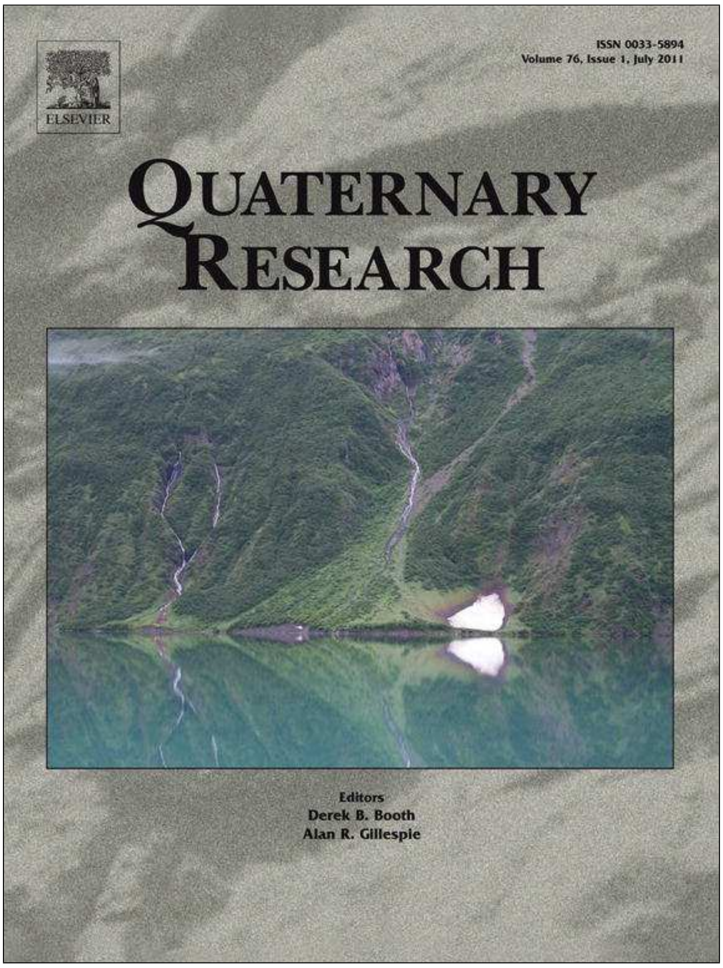
ISSN 0033-5894
Volume 76, Issue 1, July 2011
ELSEVIER
QUATERNARY RESEARCH
Editors
Derek B. Booth
Alan R. Gillespie

Quaternary Research 76 (2011) 30–45

Contents lists available at ScienceDirect

Quaternary Research

journal homepage: www.elsevier.com/locate/yqres

Holocene coastal change in the ancient harbor of Yenikapı–İstanbul and its impact on cultural history

Oya Algan [a,*], M. Namık Yalçın [b], Mehmet Özdoğan [c], Yücel Yılmaz [d], Erol Sarı [a], Elmas Kırcı-Elmas [a], İsak Yılmaz [b], Özlem Bulkan [b], Demet Ongan [a], Cem Gazioğlu [a], Atike Nazik [e], Mehmet Ali Polat [f], Engin Meriç [g]

[a] *İstanbul University, Institute of Marine Sciences and Management, Vefa, 34116, İstanbul, Turkey*
[b] *İstanbul University, Engineering Faculty, Department of Geological Engineering, Avcılar 34850, İstanbul, Turkey*
[c] *İstanbul University, Faculty of Letters, Department of Archaeology, Beyazıt, İstanbul, Turkey*
[d] *Kadir Has University, Cibali Campus, Haliç, İstanbul, Turkey*
[e] *Çukurova University, Faculty of Engineering and Architecture, Department of Geological Engineering, Balcalı, TR-01330 Adana, Turkey*
[f] *İstanbul Arkeoloji Müzesi, Gülhane, İstanbul, Turkey*
[g] *Moda, Hüseyin Bey Sokak No:15/4, 34710, Kadıköy, İstanbul, Turkey*

ARTICLE INFO

Article history:
Received 2 July 2010
Available online 12 May 2011

Keywords:
Eastern Mediterranean
Sea of Marmara
İstanbul
Ancient harbor
Coastal sediments
Holocene transgression
Neolithic
Geoarchaeology

ABSTRACT

An extensive rescue excavation has been conducted in the ancient harbor of İstanbul (Yenikapı) by the Sea of Marmara, revealing a depositional sequence displaying clear evidence of transgression and coastal progradation during the Holocene. The basal layer of this sequence lies at 6 m below the present sea level and contains remains of a Neolithic settlement known to have been present in the area, indicating that the sea level at ~8–9 cal ka BP was lower than 6 m below present. Sea level advanced to its maximum at ~6.8–7 cal ka BP, drowning Lykos Stream and forming an inlet at its mouth. After ~3 cal ka BP, coastal progradation became evident. Subsequent construction of the Byzantine Harbor (Theodosius; 4th century AD) created a restricted small basin and accumulation of fine-grained sediments. The sedimentation rate was increased due to coastal progradation and anthropogenic factors during the deposition of coarse-grained sediments at the upper parts of the sequence (7th–9th centuries AD). The harbor was probably abandoned after the 11th century AD by filling up with Lykos Stream detritus and continued seaward migration of the coastline.

Introduction

The city of İstanbul occupies a unique location in the world with respect to its geographical and historical settings. It is located at the narrow and shallow Bosporus (İstanbul Strait), which constitutes the end point of the Black Sea–Mediterranean corridor, and has coasts on both the Marmara and Black seas. Not only does its historical setting cover the time of Byzantine and Ottoman Empires, but also this location has always been of prime importance in the earlier history of civilization. From both geographical and historical points of view, it connects two marine realms and two continents as a crossroads between Anatolia and southeastern Europe (Fig. 1).

The Sea of Marmara (SOM), a part of the Black Sea–Mediterranean Corridor, is an inland sea that constitutes a geological and oceanographical link between these two basins. It was transformed into a brackish lake with the lowering of the global sea level during the late glacial period. During this period, the shelf areas of the SOM were terrestrial environments with delta progradations. These conditions turned gradually into a marine environment as a result of rising sea level at ~14 cal ka BP, from the Çanakkale (Dardanelles) Strait (Stanley and Blanpied, 1980; Aksu et al., 1999, 2002; Çağatay et al., 2000). The initial drowning of the shelf areas was interrupted by a short stillstand at −65 m during the Younger Dryas (Çağatay et al., 2003). The last reconnection with the Black Sea during the early Holocene is controversial in the published literature since 1997, with disagreement between scenarios of a continuous outflow of the Black Sea (Aksu et al., 1999, 2002; Hiscott and Aksu, 2002; Hiscott et al., 2007) or initiation with the Mediterranean transgression into the low-level Black Sea (Ryan et al., 1997, 2003; Major et al., 2006; Lericolais et al., 2007). Sea level reached present-day conditions at about ~7 cal ka BP with the drowning of various coastal depositional environments based on the faunal composition of littoral sediments from boreholes drilled at the coastal areas of the SOM (Meriç and Algan, 2007).

Problems related to cultural history further complicate a conclusive picture on the final establishment of the connection between the SOM and the Black Sea. Although the Neolithic Period, as a threshold in the history of civilization, was shown to be initiated at ~10,500–11,000 BC in certain areas of the Near East and in Central Anatolia, its dispersal to

* Corresponding author. Fax: +90 212 526 84 33.
E-mail address: algan@istanbul.edu.tr (O. Algan).

0033-5894/$ – see front matter © 2011 University of Washington. Published by Elsevier Inc. All rights reserved.
doi:10.1016/j.yqres.2011.04.002

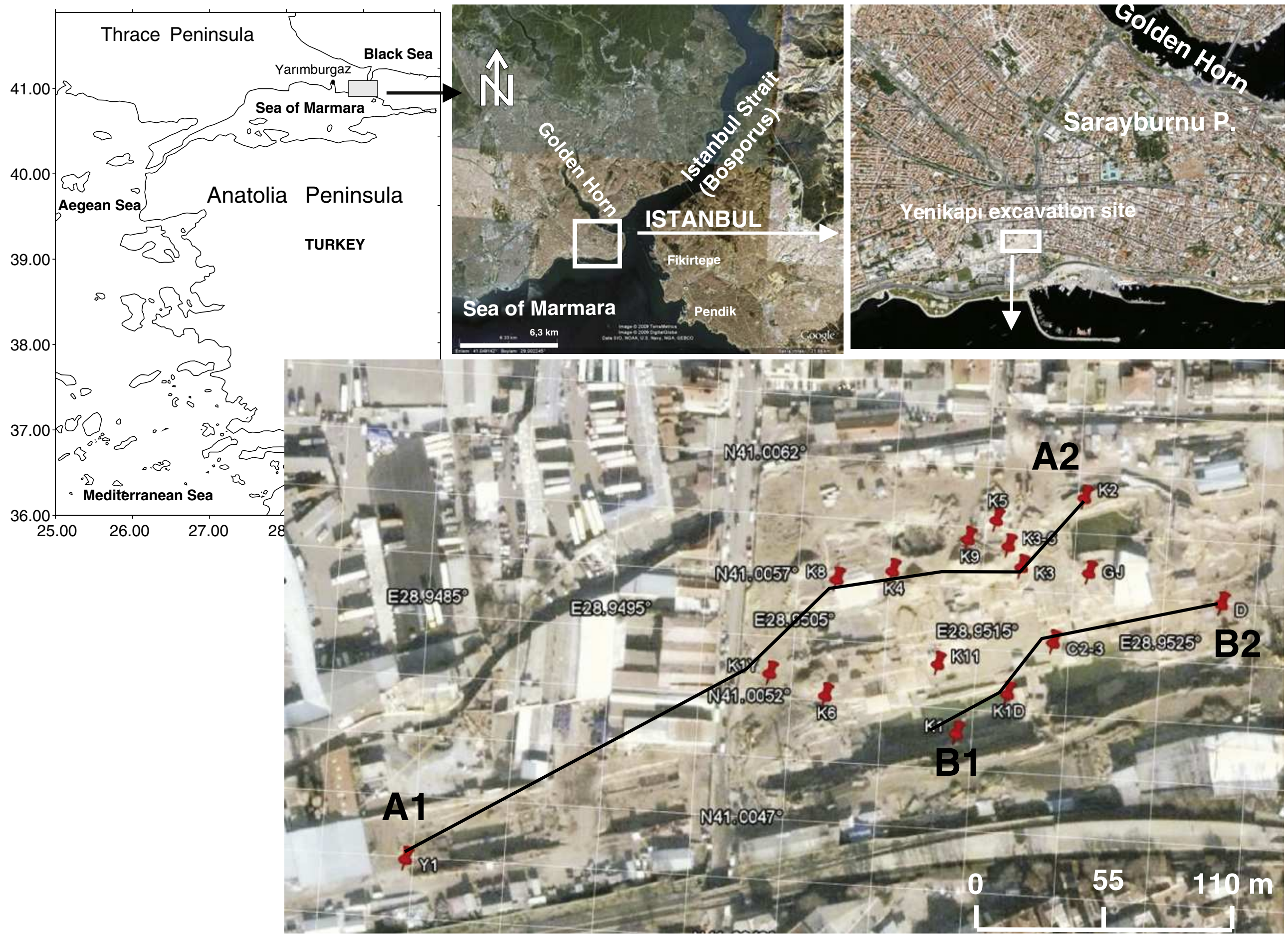

Figure 1. Location of the study area. Lines with labeled A1–A2 and B1–B2 indicate the directions of stratigraphic correlation between measured stratigraphical sections in Fig. 5. Images obtained from Google Earth 4.3.

southeastern Europe took place only by 6600–6500 BC (Pinhasi, 2003; Lichter, 2004). Due to its strategic location between Anatolia–Near East and southeastern Europe, the Marmara basin in general and more specifically İstanbul has a critical importance in our understanding the mode of this early endemic movement (Özdoğan 2008).

During the preliminary construction works of the Marmaray Tube Tunnel Project, the remnants of the ancient Theodosian Harbor (also known as the Eleutherian Harbor; Müller-Wiener, 2001) were exposed at Yenikapı by the İstanbul Archaeology Museum (IAM). This large-scale project is building a tube tunnel under the sea between the Asian and European parts of the city. After the discovery of the remnants of the Byzantine harbor, a rescue excavation was commenced by IAM (Karamut, 2007). Based on historical sources (Müller-Wiener, 2001), construction of this harbor is assigned to either the time of the Emperor Constantine I (AD 306–307) or of Theodosius I (AD 379–395).

The sedimentary sequence found at the excavation site, including the remnants of the harbor, has revealed tangible evidence for changes in sea level and environmental conditions in the SOM during the Holocene (Algan et al., 2009, 2010). At yet deeper levels, a unique assemblage of archeological material dating back to the Neolithic Period has also been discovered.

Ancient harbors of the Mediterranean Sea have attracted and been investigated by numerous researchers from different disciplines and have provided important information on coastal stratigraphy, paleogeography, sea-level changes and effects of local tectonics (Morhange et al., 2000, 2001; Sivan et al., 2001; Brückner et al., 2002; Kraft et al., 2003; Marriner et al., 2005; Galili et al., 2005; Stanley and Bernasconi, 2006; Marriner and Morhange, 2007). In this paper, we present a sedimentary sequence deposited on a coastal plain with a Neolithic settlement next to a small stream, during a rise in sea level. The study site has both geological and archeological evidence for changes in the level of the SOM and possible impacts on human culture during the Holocene. The entire sequence of harbor sediments includes anthropogenic material, which allows a high-resolution geoarcheological evaluation. The present study will also be a major contribution to the geoarchaeology of buried urban harbors (based on the classification of Marriner and Morhange, 2007) of the eastern Mediterranean.

Study area

The Yenikapı excavation site is located at the southern coast of the historic center of İstanbul within the so-called “old town of İstanbul”, which actually is a peninsula (Sarayburnu) bounded to the north by the Golden Horn and to the south by the SOM (Fig. 1). A small stream, called Bayrampaşa Deresi—ancient Lykos, had been draining into the SOM through the old “historical peninsula—Sarayburnu” area (Müller-Wiener, 2001) until the 1950s, when the bed of the stream was filled in to build a road. Its valley has a length of 5.6 km and a maximum width of 1.5 km. The excavation site corresponds to the right side of Lykos valley (Fig. 2). Recent reclamation work within this area has considerably altered the original topographical features; thus the original coastline remained ~400 m behind the present one where the rescue excavations have taken place.

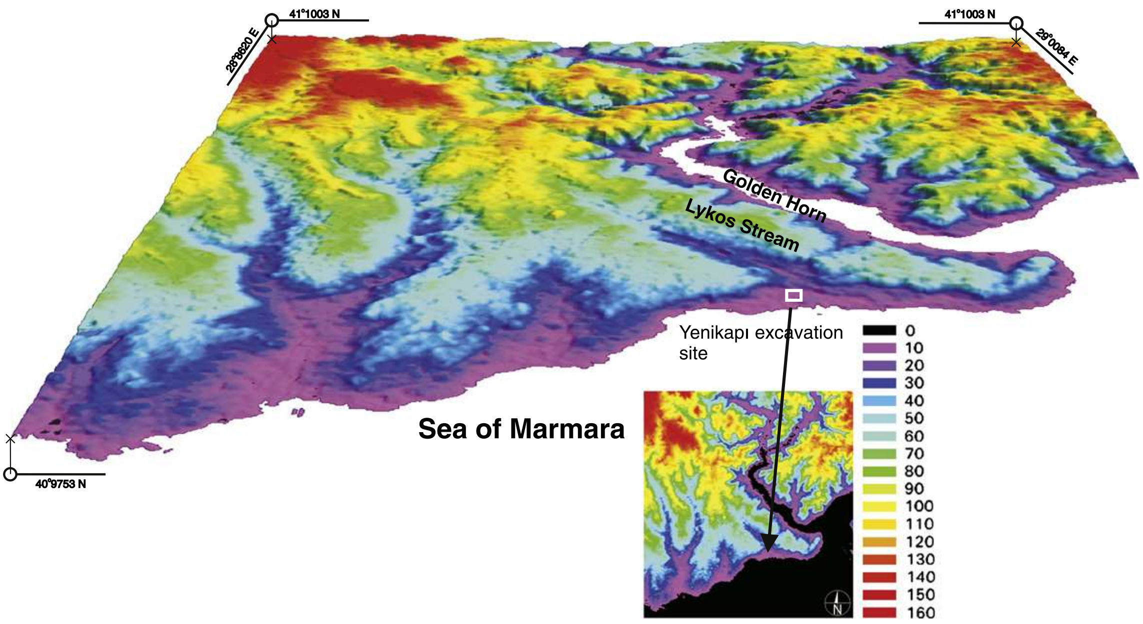

Figure 2. Three-dimensional image of the topography of the study area.

The geology of the area consists of Paleozoic and Cenozoic-age formations (Fig. 3). The Trakya formation of the Paleozoic-age is represented by sandstone, siltstone, and claystone alternations and forms the basement in the study area. Unconformably overlying Miocene-age deposits are differentiated as the Çukurçeşme, Güngören, and Bakırköy formations and constitute clastics, fine-grained and precipitated

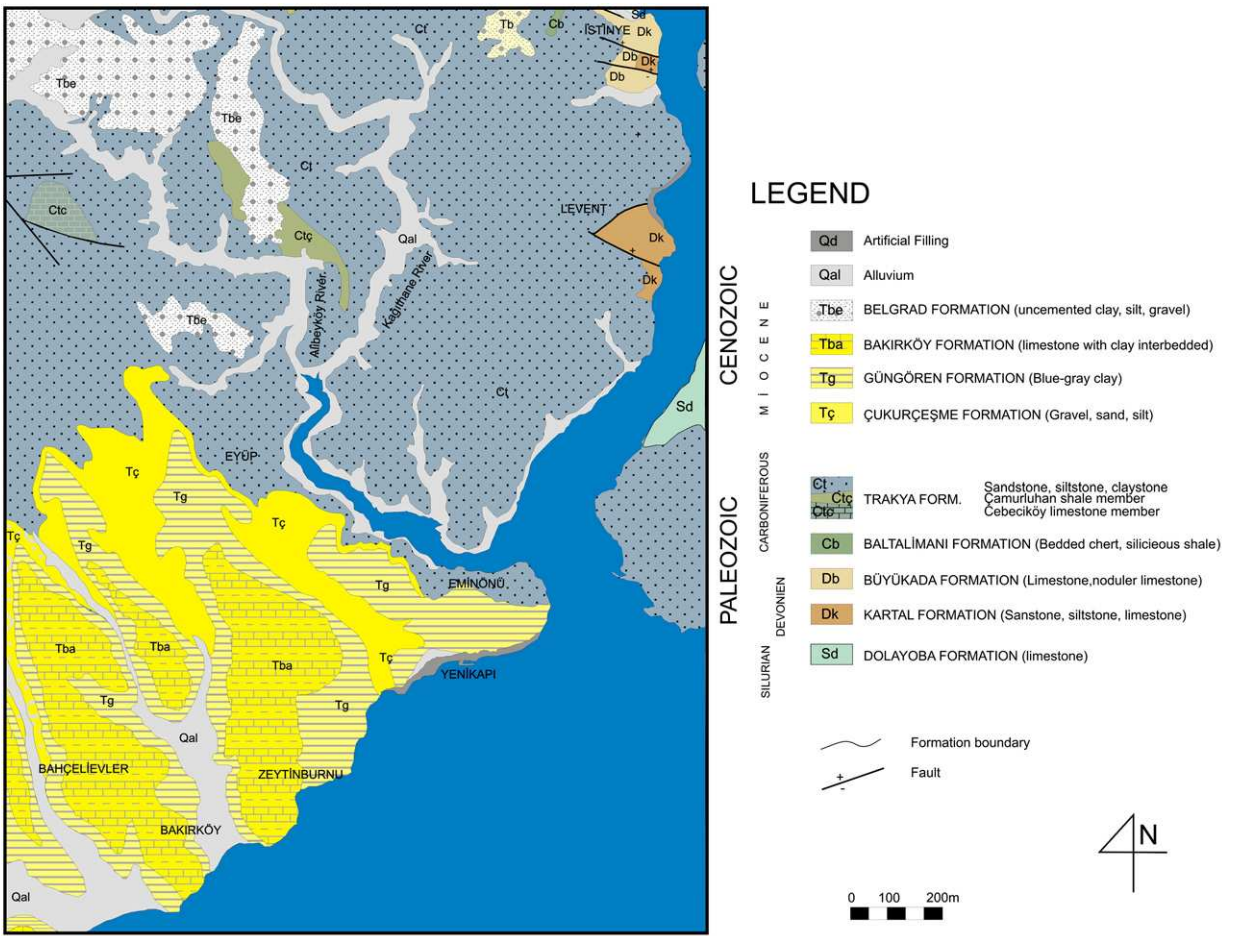

Figure 3. Geological map of the study area.
From Sayar (1977), MTA (2002) and İBB (2006).

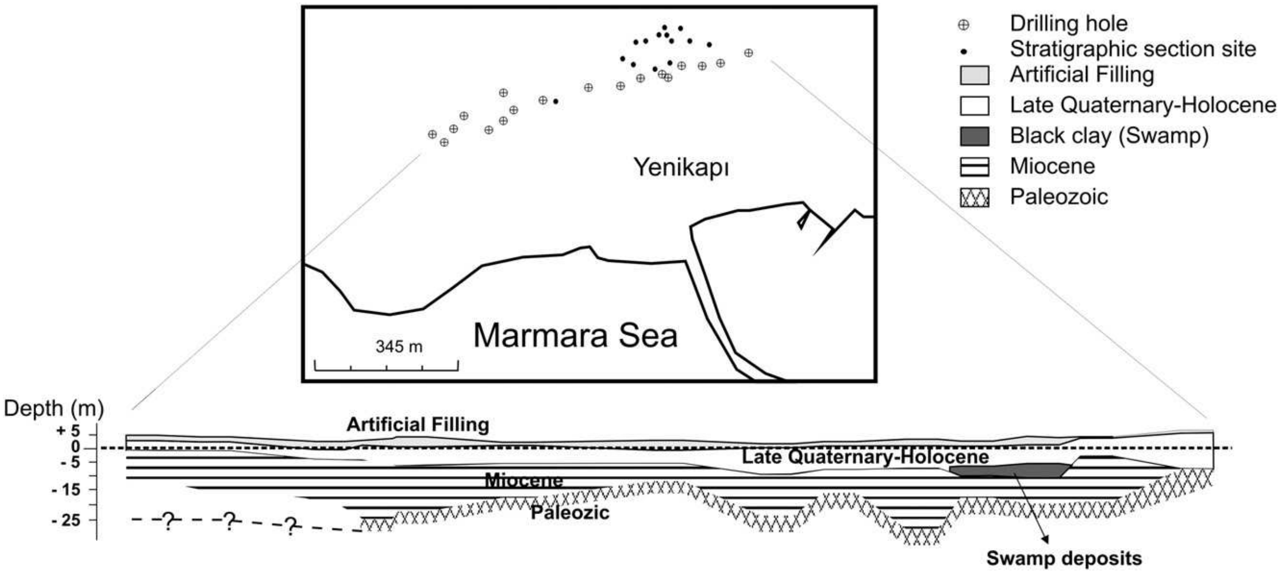

Figure 4. Generalized geological section produced from drilled boreholes. Data from MARMARAY Tube Tunnel Project (2005).

sediments, respectively, denoting a fluvial-to-lacustrine depositional environment. Alluvial deposits are limited to roughly north–south trending creek or stream valleys. Based on drill holes by the MARMARAY Tube Tunnel Project (2005) in the vicinity of the excavation site, a simplified geological section is produced (Fig. 4). Artificial filling and part of the Quaternary deposits are located above the present sea level. At the boundary of the Quaternary and Miocene deposits, a dark gray-black clay deposit is found in a small depression-like paleotopographical setting. We considered it a small swamp, formed on the floodplain of Lykos Stream along an abandoned distributary channel, as indicated by tree roots and abundant plant material (see below, section "Results").

The Marmara region is tectonically very active. The North Anatolian Transform Fault Zone (NAFZ) cuts across the region in an E–W direction, following the major axis of the SOM. In the region the

Table 1
Radiocarbon dates of the samples. Sampling depths represent the field measurements, not the ground level as in Figure. 5. SD: swamp deposits.

Lab. no	Location no/depth-cm	Units	Dated materials	^{14}C yr BP	Cal yr BP (AD and BC)	
					1σ (68.3%)	2σ (95.4%)
14912	K1/340–342	P2	Charcoal	1195 ± 100	1000–1260 (AD 690–950)	940–1290 (AD 660–1020)
14925	K1/556–561	P4	*Cerastoderma glaucum*	1635 ± 80	1050–1260 (AD 690–900)	930–1340 (AD 610–1030)
14926	K1/671–676	P4	*Cerastoderma glaucum*	1830 ± 85	1250–1480 (AD 470–700)	1200–1600 (AD 350–830)
14927	K1/771–776	P5	*Cerastoderma glaucum*	2030 + 110/− 105	1400–1700 (AD 250–550)	1300–1850 (AD 100–660)
14928	K1/786–791	P5	*Cerastoderma glaucum* + *Paphia aurea* + *Chamelea gallina*	2010 ± 125	1370–1700 (AD 260–580)	1260–1870 (AD 90–700)
14929	K1/866–871	P7	*Bittium latreilli*	3260 + 80/− 75	2910–3190 (1240–960 BC)	2780–3310 (1360–830 BC)
14930	K1/900	P7	*Glycymeris* sp.	3335 ± 55	3020–3260 (1320–1070 BC)	2900–3360 (1410–950 BC)
14931	K1/916–921 A	P7	*Paphia aurea* + *Chamelea gallina* + *Gastrana fragilis*	6015 ± 150	6250–6600 (4660–4300 BC)	6020–6770 (4830–4070 BC)
15072	K1/916–921 B (shell bank)	P7	*Chlamys* sp.	3650 ± 75	3390–3630 (1690–1440 BC)	3300–3800 (1860–1350 BC)
15073	K1/916–921 C (shell bank)	P7	*Chamelea gallina*	5915 ± 75	6190-6400 (4450–4240 BC)	6050–6500 (4590–4100 BC)
14916	C2-3 A	P7	*Ceritium vulgatum*	3085 + 125/− 120	2690–3040 (1090–740 BC)	2460–3220 (1270–510 BC)
15083	C2-3 B	P7	*Bittium latreilli*	4080 ± 95	3900–4230 (2290–1950 BC)	3760–4410 (2460–1810 BC)
AA84216	C2-3 C	P7	*Bittium latreilli*	6412 ± 43	6740–6950 (5000–4791 BC)	6650–7080 (5130–4700 BC)
AA84215	C2-3 D	P7	*Bittium latreilli*	6307 ± 49	6630–6840 (4889–4680 BC)	6510–6940 (4989–4560 BC)
AA84222	C2-3 E	P7	Sediment	6274 ± 43	7170–7251 (5302–5221 BC)	7025–7291 (5342–5076 BC)
15082	C2-3 (GJ 21/200–202)	SD	*Mytilus* sp.	7460 ± 110	7740–8010 (6060–5790 BC)	7630–8160 (6210–5690 BC)
AA84221	C2-3 (GJ 21/200–202)	SD	Sediment	7305 ± 47	8050–8170 (6221–6101 BC)	8008–8196 (6247–6059 BC)
AA84220	C2-3 (GJ23/220–222)	SD	Sediment	7592 ± 44	8372–8420 (6471–6423 BC)	8329–8510 (6561–6380 BC)
15077	D/200–205	P4	*Cerastoderma glaucum* + *Paphia aurea*	2000 ± 55	1400–1620 (AD 330–560)	1310–1730 (AD 220–640)
15075	D/335–340 A	P7	*Chlamys* sp.	3065 ± 60	2720–2910 (960–770 BC)	2580–3070 (1120–630 BC)
15076	D/335–340 B	P7	*Chamellea gallina*	6105 ± 70	6390–6620 (4670–4440 BC)	6290–6720 (4770–4340 BC)
AA84219	D (G47/70–72)	SD	Sediment	7708 ± 45	8445–8541 (6592–6496 BC)	8414–8563 (6633–6465 BC)
AA84218	D (G47/160–162)	SD	Sediment	10,090 ± 160	11,360–11,970 (10,020–9410 BC)	11,220–12,380 (10,430–9270 BC)
AA84217	D (G47/200–202)	SD	Sediment	11,770 ± 230	13,380–13,830 (11,890–11,430 BC)	13,150–14,130 (12,180–11,210 BC)
14932	K3/280–285	P3	*Chamellea gallina* + *Paphia aurea*	1670 ± 90	1060–1290 (AD 660–890)	930–1400 (AD 550–1020)
14933	K3/342–354	P4	*Cerithium vulgatum*	1825 ± 100	1230–1490 (AD 460–720)	1070–1600 (AD 340–880)
14934	K3/455–460	P5	*Cerastoderma glaucum*	1920 ± 95	1300–1550 (AD 400–650)	1210–1720 (AD 230–740)
14924	K3/470–475	P5	*Cerastoderma glaucum*	2195 ± 95	1600–1880 (AD 70–350)	1470–2040 (100–490 BC)
15074	K3/750–755	P7	*Ostrea*	5475 ± 70	5700–5910 (3970–3750 BC)	5580–6030 (4080–3640 BC)

rate of right-lateral offset along the NAFZ has been measured to be about 18 mm/yr (Flerit et al., 2003; Pondard et al., 2007). The NAFZ is widely known to have generated large earthquakes (M>7) at 125–150 yr intervals. In the Düzce and Gölcük (Izmit) earthquakes of 1999, the lateral offset along the fault locally exceeded 5 m (Toksöz et al., 1999; Reilinger et al., 2000). The İstanbul area is a fault block bounded on the south by the NAFZ and on the north by the South Boundary Fault of the Black Sea Basin (Yılmaz, 2007; Yılmaz et al., 2010). This fault-bounded block is forced to rotate anticlockwise due to the sinistral shear. This rotation is expressed clearly in the geomorphology; major hills and the valleys trend obliquely to the two faults, following a long way before reaching the surrounding seas. Simultaneously with the anticlockwise rotation, the fault block has been elevated at a rather slow rate of about 0.2 mm/yr. However, these tectonically induced slow vertical motions have not caused radical changes in the study area during the recent 8000–10,000 yr period. But, some more remarkable local vertical movements caused by the activities of the NAFZ cannot be ruled out.

Methods

Measurements of stratigraphical sections were carried out in 16 locations at the excavation site (Fig. 1), including lithological observation and sampling at less than 5-cm intervals. In some of these excavation sections (such as, K1Y, K8, K11 and C2-3) measurements of the stratigraphic sequences were not completed down to basement and/or for the upper parts, due to the fast timetable of this rescue excavation program. However, later it became possible to adequately correlate the results obtained either by direct observations or by measurement of the completed and uncompleted sections; the results were also confirmed through radiocarbon dates. Grain-size distribution of the selected samples was performed with sieve analysis and SediGraph, for coarse (>63 μm) and fine-grained (<63 μm) fractions, respectively. Mean (M, φ) and sorting values were calculated according to Folk and Ward (1957). The presence of benthic foraminiferal fauna is determined in the sediment fraction above the 63-μm sieve. About 10 g of dry samples were soaked in water for 24 h,

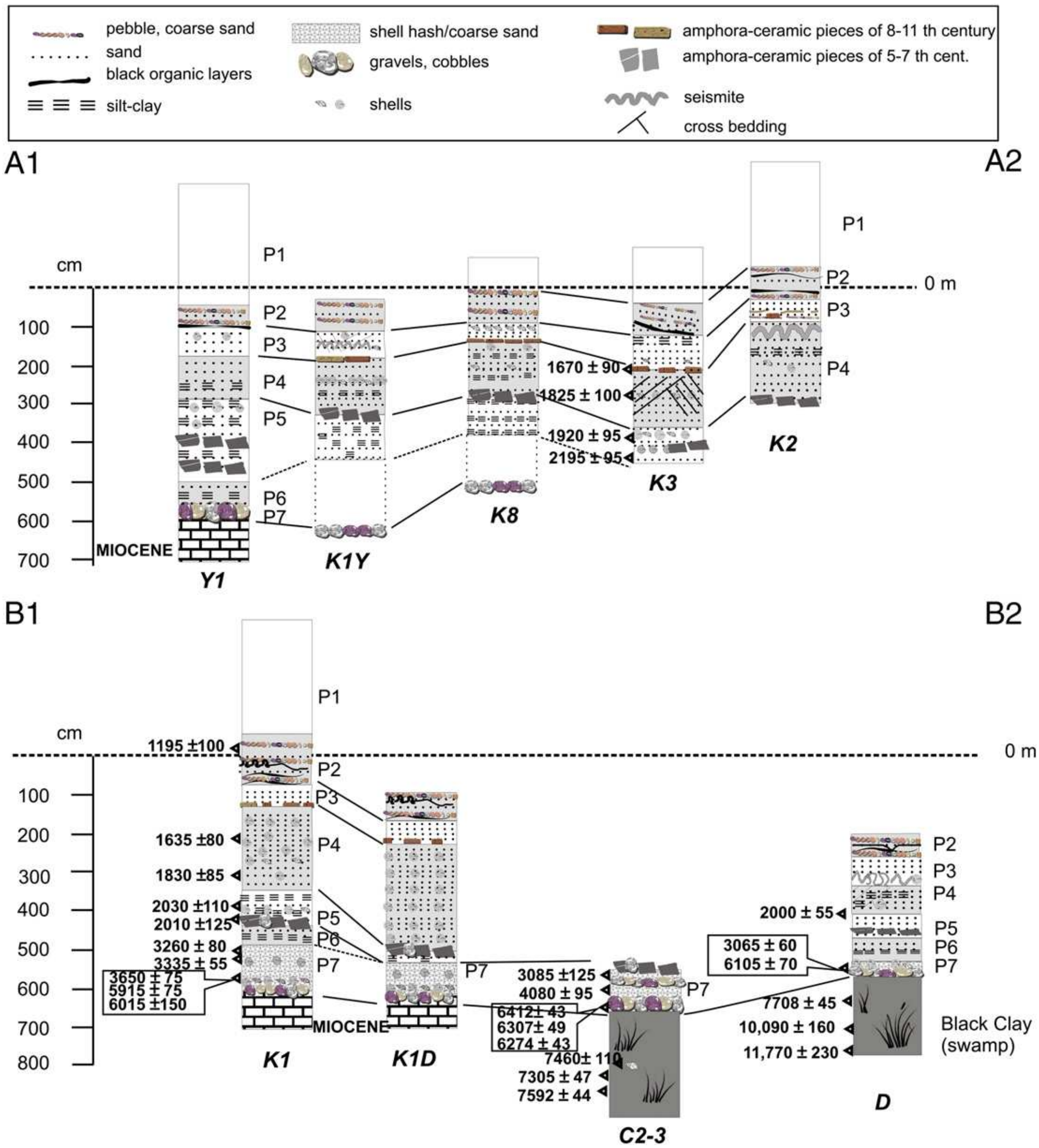

Figure 5. Lithological and stratigraphical correlations of measured sections through lines A and B shown in Fig. 1. Dates (e.g., 1635 ± 80) are given as uncalibrated years BP (see Table 1). Part of the sections shown with dashed lines (in K1Y and K8) was drawn on the base of ground level of gravels and cobbles.

and then wet sieved through a 63-μm sieve. The residue from the sieve was dried in air and split with a microsplitter, until a subsample containing a minimum of 300 benthic foraminiferal specimens was obtained. Benthic foraminiferal specimens were counted under a binocular microscope. For ostracod fauna, approximately 10 g of dry sediment was washed through a 63-μm sieve. The residue was then air-dried and sieved at 125 μm; all ostracods retained on the sieve were picked out under a binocular microscope and transferred onto slides before identification. Ostracod determinations and their salinity tolerance were based on definition of Van Morkhoven (1963), Breman (1975), Guillaume et al. (1985) and Meisch (2000). Species were evaluated according to their relative abundances in the samples.

Radiocarbon dating of the selected mollusc samples was carried out at the Environmental Isotope Laboratory and AMS Laboratory of Arizona University (USA) (Table 1). Radiocarbon ages were calibrated using Calib Rev 5.1. Beta (Stuiver et al. 2005) with reservoir age (for shell samples) correction of 390 ± 85 yr with ΔR 35 ± 70 yr (Siani et al., 2000). Marine04 and IntCal04 curves were used for shell samples and charcoal and sediment samples, respectively. The dating of the prehistoric archeological material was through comparing the Yenikapı assemblage with previously studied material from other sites in the Marmara region (Özdoğan, 1997, 2006, 2007).

Results

Lithostratigraphy of the sedimentary sequence

Based on stratigraphical measurements and lithological characteristics in a total of 16 locations, two main types of sedimentary sequences are differentiated below the artificial fillings (Fig. 5; Algan et al., 2007, 2009). The artificial fillings (P1) have debris from the Byzantine period, organic soil of Ottoman period, and constructional

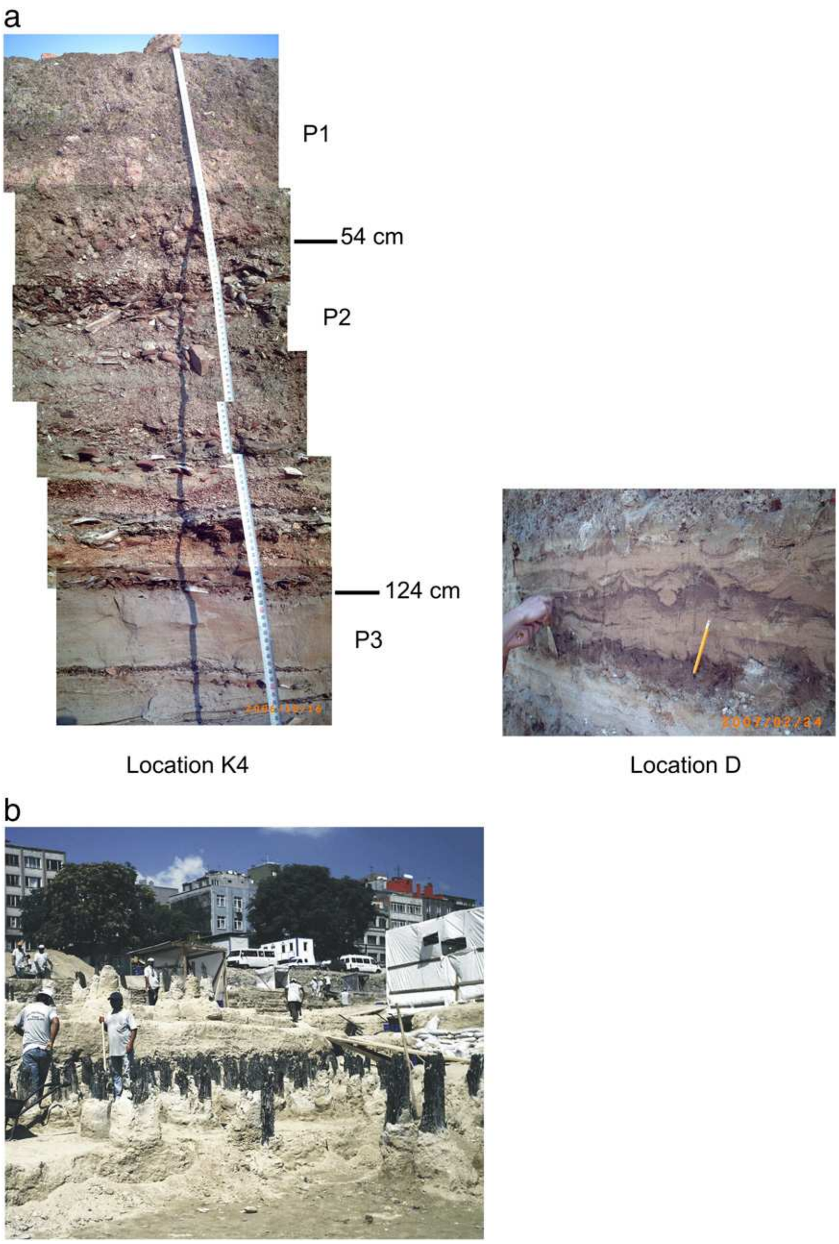

Figure 6. Photos indicating (a) lithological characteristics of units P1, P2 and P3 from location K4 and seismite-type bedforms in location D; (b) wood piers of the Byzantine Harbor in Unit P4; (c) chaotic deposit of unit P5 in location K1; (d) units P5 and P6 from location D; (e) unit P7 in different locations—arrows indicate the shell hash and coarse grained shelly sands; (f) boundary between unit P7 and swamp deposit, close to locations K2. The size of the scale in (c and d): red or white bands are 20 cm in length.

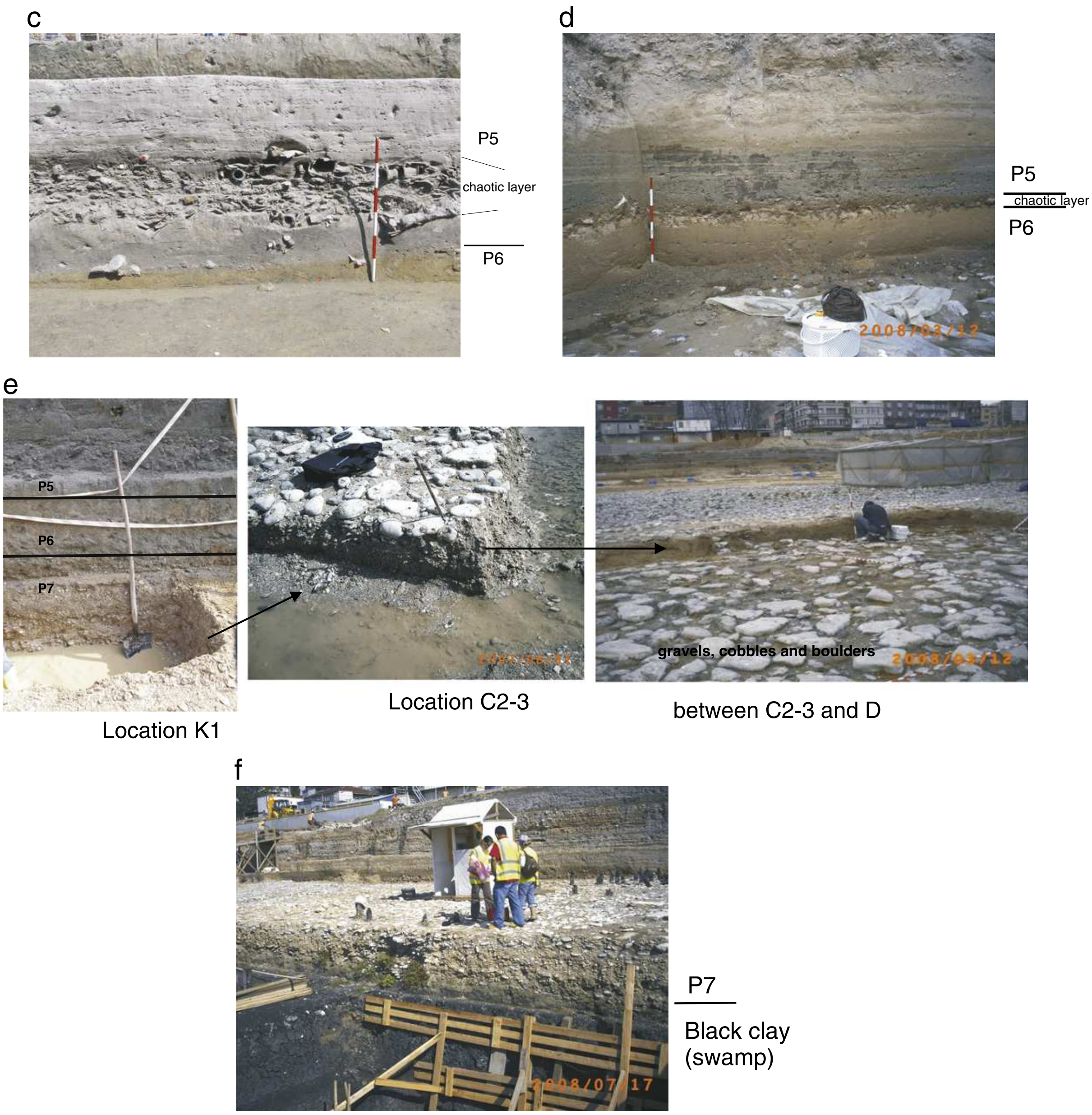

Fig. 6 (*continued*).

concretes of the 20th century. The fluvial–deltaic sedimentary sequence (P2) below the artificial fillings has a thickness of about 1 m. It is mainly represented by coarse grained sediments and was deposited from the detritus of Lykos Stream. The marine sequence consists of five different units (P3–P7) and overlies both the basement and a local swamp deposit (Fig. 5).

A fluvial–deltaic sequence P2 consists of alternating graded and non-graded yellow-brownish coarse-grained sediments (Fig. 6a), as depicted in the grain size distribution diagram (Fig. 7). Sandy gravels are intercalated by coarse sands. Sorting values show mostly “poorly” and/or “very poorly” sorted, for the gravelly layers and becomes better with the increasing sand content. Abundant broken and rounded pottery sherds, artifacts, bones, and shells—evidently food residues—are found within the layers of this unit (Fig. 6a). These anthropogenic components reflect a time period between the 8th and 11th centuries AD, based on the ceramic typology. Between these coarse grained layers, black charcoal and other organic inclusions are found as discrete thin layers. These changes in the lithology and grain-size distribution of this sequence might be related to the flow regime of Lykos Stream influenced by short-term climatic changes, but anthropogenic activities (such as agriculture, urban constructions, and fires on the drainage area during Byzantine times) must also have had an impact. A small distributary channel in a SSW to NNE direction is also observed at the site, incised into the underlying marine sequence. Its fill material is mainly thick (10–13 cm) black charcoal and sandy gravelly layers.

The boundary between the P2 and marine sequence is sharp (Fig. 6a). P2 bevels with a very low angle over P3. The uppermost marine unit P3 constitutes of homogeneous beige-color sands with local cross bedding and silty-clay bands. Mean (M) grain size of sands is medium to fine sand (2–3φ) (Fig. 7). It is well-sorted (sorting value: 0.4) with the exception of the thin silty-clay layers. Within the fine-grained bands, some seismite-type bedforms are observed (Fig. 6a). These soft sediment deformation structures are believed to have resulted from an instantaneous segregation of the liquid from the solid sedimentary phase by a seismic shock. The thickness of P3 varies from 50 to 120 cm, and is thickest in location K2 (Fig. 5).

Unit P4 is lithologically quite similar to P3 but includes shells, as scattered and also as discrete layers. It is finer ($M = 3\varphi$) and poorly

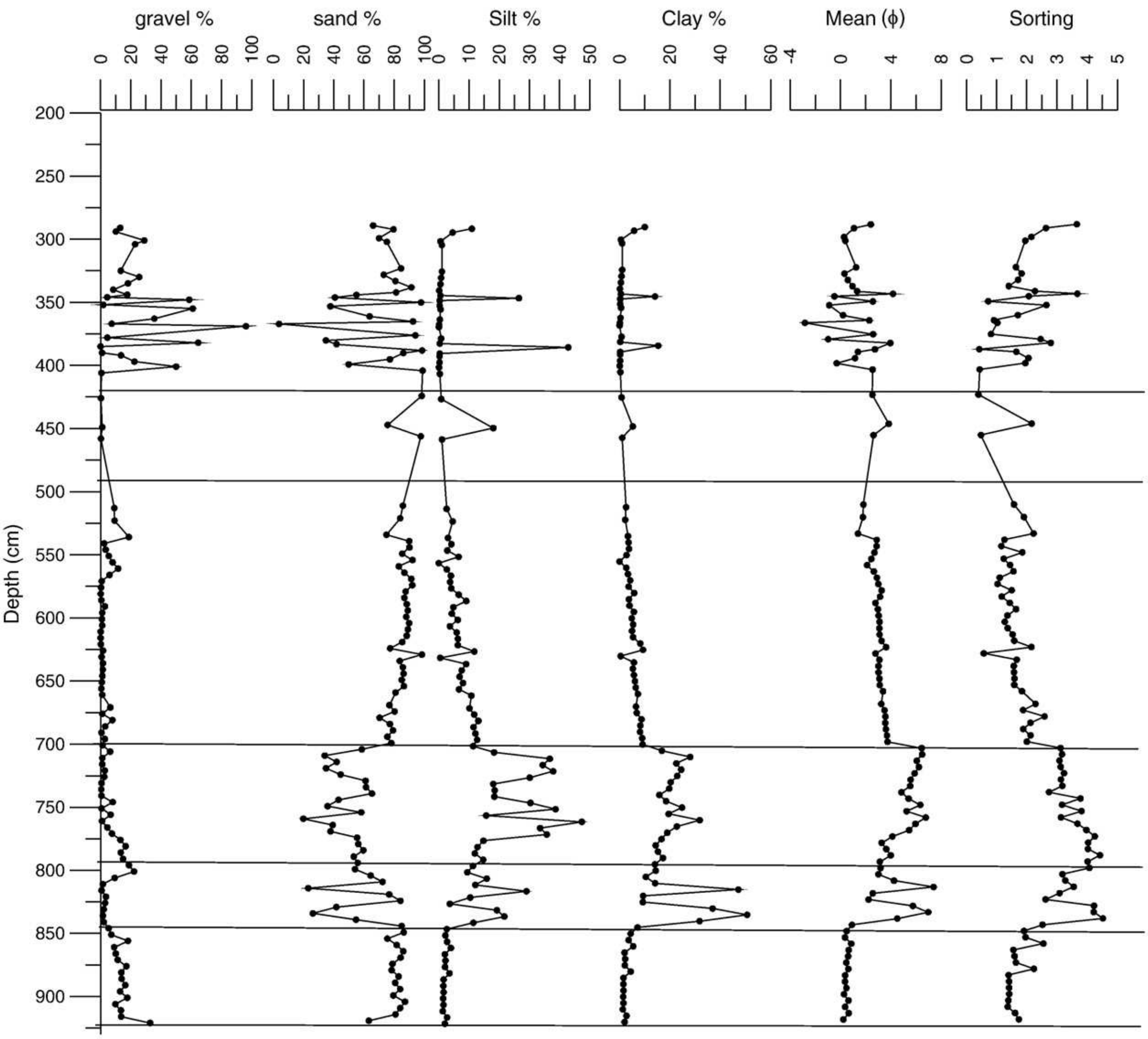

Figure 7. Grain-size distribution and textural parameters of the samples from location K1.

sorted, compared to P3 (Fig. 7) and has a thickness ranging between 65 and 300 cm (Fig. 5). Likewise with P3, it contains local cross bedding, brownish silty-sand bands and layers, particularly in the northern locations (K2, K8, K6, Y1, and D). Within this unit, more than 30 sunken ships, wrecks and wood pilings (Fig. 6b) of the Byzantine harbor were found (Pulak, 2007; Kocabaş, 2010).

The boundary between P4 and P5 is gradual. P5 consists of silty-clayey sands and a considerable amount of anthropogenic artifacts (Fig. 6c). Its fine-grained component decreases northward and eastward, as it is represented by sands in location D. Its thickness is variable and almost 200 cm in location Y1, thinning out towards the north (Fig. 5, compare K1D and K8). Sorting values become very poor, and extremely poor within P5 (Fig. 7). A chaotic anthropogenic deposit with abundant broken fragments of pottery vessels, bones, marble blocks, coins, and broken glass was found in this unit at locations Y1, K1, K1D, K1Y, and K8. The ceramics and amphoras belong to the 5–7th centuries (Fig. 6c). This chaotic deposit is widespread in the excavation site, as observed at the base of unit P4 at locations K9 and D, and has a thickness of 116 cm in location Y1, thinning to less than 20 cm eastwardly in location D (Fig. 6d). Its origin was associated with a tsunami event caused by the AD 553 or 557 İstanbul earthquakes (Perinçek, et al., 2007; Perinçek, 2010). On the other hand, continuing archeological examination of the Byzantine materials within this deposit close to the location Y1 indicates an undisturbed stratigraphy for the time interval from ~AD 500 to 700. This chaotic material likely reflects dumping materials from harbor activities and ships within the Byzantine breakwater. It also might have been formed by a strong flood event. The origin of this chaotic deposition (tsunami, flood, or anthropogenic activities) is still not clear and will be understood only after completion of the archeological evaluation and more detailed geological analysis in the nearby coastal area.

P6 is a light yellowish sandy unit and includes locally small-scale cross bedding and thin fine-grained yellow-brown clay bands (Figs. 6c and d, and 7). P7 has maximum 1-m thickness in the south thinning northwardly, and is represented by coarse sandy shell hash (Fig. 5). These coarser grained sediments laterally change to gravel clusters intercalated by coarse sands at and in the vicinity of location C2-3 (Figs. 6e and f). At location K1 and K1D, a shell bank locally forms its base but does not continue away from K1D. It was previously defined as unit P8 in Algan et al. (2009); however, further observation together with the progression of the excavation at the site and more radiocarbon dates made clear that they belong to same unit with laterally changing facies. Shell hash content of P7 thins out towards east and north.

Gravels and cobbles underlie the marine sequence and are considered to be the base of P7 (Fig. 6e). The clastic materials are mostly well-rounded and the cobbles, derived from the Paleozoic and

Table 2
List of genera and species of benthic foraminifera found in different locations of the excavation site (see Figs. 1 and 5).

Foraminifer	K1	K2	Y1	C2-3	D
Ammoscalaria runiana (Heron-Allen & Earland)	X		X		
Spirillina vivipara Ehrenberg	X	X	X	X	X
Patellina corrugata Williamson	X			X	X
Ophthalmidium sp.					X
Adelosina carinata-striata Wiesner	X	X	X	X	X
A. cliarensis (Heron-Allen & Earland)	X				
Adelosina sp.	X				
Adelosina spp.	X				
Fillinita spp.	X				
Spiroloculina dilatata d'Orbigny	X				
S. excavata d'Orbigny	X				
Spiroloculina sp.	X				
Spiroloculina spp.	X				
Siphonaperta aspera (d'Orbigny)	X			X	X
S. irregularis (d'Orbigny)				X	
Siphonaperta spp.	X			X	
Cycloforina contorta (d'Orbigny)	X	X	X	X	X
Cycloforina sp.	X		X	X	
Massilina gualtieriana (d'Orbigny)	X			X	
M. secans (d'Orbigny)	X	X	X	X	X
Massilina sp.	X			X	
Quinqueloculina annectens (Schlumberger)	X		X		
Q. berthelotiana d'Orbigny	X			X	X
Q. bidentata d'Orbigny	X	X	X	X	
Q. bosciana d'Orbigny	X			X	X
Q. disparilis d'Orbigny	X				
Q. laevigata d'Orbigny	X	X	X		
Q. lata Terquem				X	
Q. limbata d'Orbigny	X			X	
Q. oblonga	X	X	X	X	X
Q. parvula Schlumberger	X			X	
Q. seminula (Linnaeus)	X	X	X	X	X
Q. stalkeri Loeblich & Tappan				X	
Q. stelligeria Schlumberger	X				
Quinqueloculina sp.				X	
Quinqueloculina spp.	X	X	X	X	X
Miliolinella circularis-elongata Kruit	X				
M. labiosa (d'Orbigny)	X				
M. subrotunda (Montagu)	X	X	X		X
Miliolinella sp.	X				
Miliolinella spp.	X				
Pseudotriloculina cuneata (Karrer)			X	X	
P. laevigata (d'Orbigny)	X	X	X	X	X
P. oblonga (Montagu)	X				
Pseudotriloculina rotunda (d'Orbigny)	X		X		
Pseudotriloculina sp.	X		X	X	
Pyrgo elongata (d'Orbigny)	X				
Triloculina bermudezi Acosta	X				
T. marioni Schlumberger	X				
Sigmoilinita distorta (Phleger & Parker)	X	X	X		
S. costata (Schlumberger)	X			X	X
Sigmoilinita sp.	X			X	X
Parrina bradyi (Millett)	X				
Brizalina spathulata (Williamson)				X	
B. striatula (Cushman)				X	
Brizalina sp.	X		X		
Bulimina aculeata d'Orbigny				X	
Stomatorbina concentrica (Parker & Jones)	X				
Stomatorbina sp.	X				
Neoconorbina terquemi (Rzehak)	X			X	
Rosalina bradyi Cushman	X	X	X	X	
R. globularis d'Orbigny	X				
Rosalina floridensis (Cushman)				X	X
Rosalina sp.	X		X	X	
Rosalina spp.					X
Glabratella sp.	X				
Cibicidoides sp.	X		X	X	
Discorbinella bertheloti (d'Orbigny)				X	
Lobatula lobatula (Walker & Jacob)	X			X	X
Asterigerinata adriatica Haake	X	X	X		
A. mamilla (Williamson)	X			X	
Nonionella turgida (Williamson)				X	
Astrononion sp.				X	X
Aubignyna perlucida (Heron-Allen & Earland)	X				
Aubigyna sp.	X				
Ammonia compacta (Hofker)	X		X	X	X
A. parasovica Stschedrina & Mayer	X	X	X	X	X
A. parkinsoniana (d'Orbigny)	X	X	X	X	X
A. tepida (Cushman)	X	X	X	X	
Ammonia sp.				X	
Ammonia spp.	X			X	
Cribroelphidium poeyanum (d'Orbigny)	X			X	X
Porosononion subgranosum (Egger)	X	X	X	X	X
Elphidium aculeatum (d'Orbigny)	X	X	X	X	X
E. advenum (Cushman)	X			X	
E. complanatum (d'Orbigny)	X	X	X	X	X
E. depressulum Cushman	X				
E. gerthi van Voorthuysen	X		X	X	X
E. macellum (Fichtel & Moll)	X	X	X	X	
E. pauciloculum (Cushman)	X	X	X	X	X
E. cf. *pulvereum* Todd	X		X		
Elphidium spp.	X	X	X	X	X
Haynesina depressula (Walker & Jacob)	X	X	X	X	X
Haynesina sp.	X			X	X
Haynesina spp.	X				

Cenozoic units of the İstanbul area, contain burrows made by marine organisms. These deposits are spread out onto the Miocene-age formations, but also onto the dark gray-blackish clay deposits of a swamp, where they are well-packed, display slight orientation and contain sands and large shells (Fig. 6f). There are also angular boulders and large cobbles mainly in the south extension of the excavation site. Their rectangular shapes and large sizes suggest that they were brought from a nearby area by humans, rather than transported by waves, currents, and riverine input.

The thickness of the swamp clay is about 7–8 m, and its circular external form has a radius of about 250 m, based on drilling data (Fig. 4). Besides containing several wood pieces and big tree roots, a few cremations and urn-type burials were also recovered in its external parts.

Chronology of the sedimentary sequence

The radiocarbon age obtained from unit P2 (1195 ± 100 ^{14}C yr BP; AD 690–950, Table 1) is in agreement with 8th century ceramics found in the same unit. Various mollusk shells yielded ages spanning a period from ~AD 70–890 (~1.1 to 1.9 cal ka BP, Table 1) for units P3, P4, and P5. Regarding these ages, the sedimentation rate appears to be higher during the deposition of these units (between 0.39 and 0.26 cm/yr from location K1), compared to P7 (0.15–0.25 cm/yr). This rate is higher than the rates estimated for the ancient harbor of Tyre (0.1 cm/yr, Marriner and Morhange, 2006a; Marriner et al., 2008), but lower than for the ancient Roman harbor in the Tiber Delta (4 cm/yr, Goiran et al., 2010) and the ancient harbor of Marseilles (2.2 cm/yr; Morhange et al., 2003).

Small (juvenile) shells of *Bittium latreilli* in the shell hash/coarse sand facies of P7 and large individual specimens from a shell bank yielded ages of either ~3–4 cal ka BP or ~6–6.9 cal ka BP (Table 1). This is particularly notable at location D where two samples from the same interval of Unit P7 had ages of 3065 ± 60 ^{14}C yr BP and 6105 ± 70 ^{14}C yr BP. Similar ages also were obtained at 916–921 cm intervals of location K1 (3650 ± 75 ^{14}C yr BP, 6015 ± 150 ^{14}C yr BP). In location C2-3 where P7 is relatively thick (~100 cm), 4080 ± 95 ^{14}C yr BP was also obtained at about 45 cm. Previously, finding of ages ~3.3 and 6.6 cal ka BP within a very tiny interval of P7 in one location has been tentatively implied to a time gap caused by a regression (Algan et al., 2009). However, with the additional radiocarbon age determinations and the assessment of the data from other locations, a different interpretation is achieved (see Discussion section below).

Shells collected from location C2-3, close to the boundary between unit P7 and the swamp deposits yielded ages of 6412 ± 43 ^{14}C yr BP

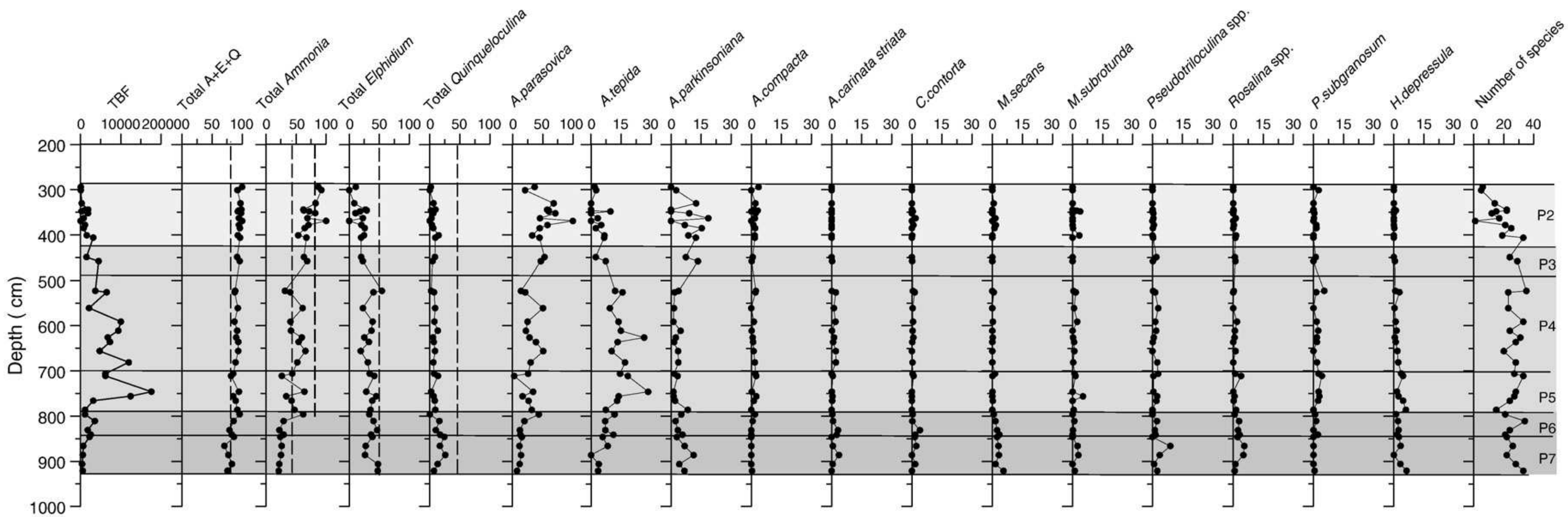

Figure 8. Vertical distribution of foraminiferal taxa with contents of only >3% from location K1. Values indicated in X axis are percentage in total. TBF = total benthic foraminifera. Total A + E + Q = Total *Ammonia*, *Elphidium* and *Quinqueloculina* species. Vertical dashed lines are used to compare the changing relative abundances between lithological units. Gray shading reflects the main changes in foraminiferal assemblages.

and 6307 ± 49 ^{14}C yr BP (Table 1, Fig. 5) whilst 6274 ± 43 ^{14}C yr BP was obtained from a sediment sample at the uppermost part of the swamp deposit. Small age differences between shells and the sediment sample might be related to the old carbon in the shells. The time for the boundary between P7 and the swamp deposit can be assigned to ~6.7–7.2 cal ka BP. Dated sediment samples from the swamp deposit range from 7305 ± 47 to 11,770 ± 230 ^{14}C yr BP (~8 to 13.8 cal ka BP; Table 1).

Benthic faunal content of the sedimentary sequence

Foraminiferal taxa determined in the study area (Table 2) are characterized by the dominance and abundance of three genera; *Ammonia*, *Elphidium* and *Quinqueloculina*. They form more than 70% of the total fauna throughout the sedimentary sequence (Fig. 8). The other genera such as, *Adelosina*, *Cycloforina*, *Massilina*, *Miliolinella*, *Pseudotriloculina*, *Rosalina*, *Porosononion* and *Haynesina* constitute the "minority group". The vertical distribution of *Ammonia* has an increasing trend towards the upper part of the section, whereas *Elphidium* and *Quinqueloculina* have a decreasing trend.

Foraminiferal fauna of unit P2 display low diversity (average species number is 16) and population. An *Ammonia*-dominated fauna, consisting of *A. parasovica*, *A. parkinsoniana*, *A. tepida* and *A. compacta* occurs in this unit with the dominance of *A. parasovica* which constitutes more than 50%. *Ammonia* species together with *Elphidium* and *Quinqueloculina* specimens represent an average 97% of the assemblage (Fig. 8, see dashed vertical line in graph Total A + E + Q). Diversity starts to increase close to the boundary of units P2 and P3, whereas total benthic foraminifera essentially increase in unit P4 and display a maximum in unit P5. *A. parasovica* displays a decreasing trend in units P3 to P5; however, its abundance is higher than the others. *A. tepida* has an increasing trend in these units, compared to

Table 3
List of genera and species of ostracoda found in two locations of the excavation site (see Figs. 1 and 5).

Location/ sampling depth	Marine										
	Aurila convexa	*Paracytheridea depressa*	*Urocythereis oblonga*	*Pontocythere elongata*	*Semicytherura inversa*	*Semicytherura sulcata*	*Callistocythere intricatoides*	*Carinocythereis carinata*	*Hiltermannicythere turbida*	*Pseudocytherura calcarata*	*Loxoconcha elliptica*
K1/cm											
289–294											
344–346	*										
352–355		*				*	*				
378–382	*		*				*				
385–390		*	*	*	*	*					*
421–426	*		*								
453–458	*	*	*	*	*		*	*			
506–513	*	*	*				*		*		*
536–541	*	*	*	*	*		*		*		
546–551	*	*	*		*			*	*	*	*
561–566		*	*	*	*		*			*	*
571–576	*	*	*		*		*	*	*	*	
581–586	*	*	*	*	*		*	*		*	
591–596	*	*	*		*	*	*		*		*
601–606	*	*	*	*	*	*	*		*	*	*
611–616	*	*	*		*		*		*		
621–626	*	*	*			*	*	*	*	*	
631–636	*	*	*	*	*	*			*	*	
641–646		*	*		*	*	*		*	*	
656–661	*	*	*	*	*	*	*		*	*	
666–671	*	*	*	*	*	*	*		*	*	
681–686	*	*	*	*		*	*		*		
691–696	*	*	*	*	*	*			*	*	
696–701	*	*	*	*		*		*	*	*	
701–706	*	*	*	*	*	*		*			
711–716	*	*	*	*	*	*	*	*			
721–726	*	*	*	*			*	*	*	*	
731–736	*	*	*	*	*	*	*	*	*		
741–746	*	*	*		*	*	*	*		*	
756–761		*	*	*	*	*	*	*	*	*	
771–776		*	*	*		*					
786–791		*		*		*					
796–801		*	*	*		*	*	*			
801–806			*	*		*	*		*		
811–816	*		*	*		*	*				
821–826	*	*	*	*	*	*	*		*		
831–836		*	*	*		*					
841–846	*	*	*			*					
851–856	*		*	*							
861–866	*		*	*	*	*					
871–876		*	*	*		*					
881–886	*		*			*					
891–896			*	*							
901–906			*			*				*	
911–916		*	*	*							
916–921			*	*						*	
GJ/cm											
70–75											
100–105											
150–155											

unit P2. *Elphidium* and *Quinqueloculina* species, such as *E. aculeatum*, *E. macellum*, *E. complanatum*, *E. advenum*, *E.* cf *pulvereum* and *Q. seminula* are also significantly abundant. *Haynesina depressula* and *Porosononion subgranosum* occur sporadically with low specimens. Total benthic foraminifera (TBF) decrease in units P6 and P7. The foraminiferal assemblage is slightly different in these two lowermost units than the upper units. Total *Elphidium*, *Ammonia* and *Quinqueloculina* decrease from about 94% to 80%. *Elphidium* species become relatively dominant against *Ammonia*. The abundance of *Quinqueloculina* and "minority group" species, including mainly *Adelosina carinata striata*, *Cycloforina contorta*, *Massilina secans*, *Pseudotriloculina* spp. and *Rosalina* spp. show a relative increase. The lateral continuation of this assemblage is recognized at locations C2-3, Y1 and D (Table 2).

From the dominant foraminifers, *Ammonia* and *Elphidium* species tolerate salinity conditions from hyposaline to hypersaline on the inner shelf, in lagoons and on tidal flats (Murray, 1973). *A. compacta*, *A. parkinsoniana*, *A. tepida*, *E. aculeatum*, *E. advenum*, *E. complanatum* and *E. macellum* occur abundantly in infralittoral (0–50 m), upper circalittoral (50–100) in the Aegean Sea (Meriç et al., 2004), Gulf of Napoli (Sgarrella and Moncharmont-Zei, 1993), Adriatic Sea (Jorissen, 1988), and Gulf of Izmit (SOM) (Meriç et al., 1995). *Quinqueloculina seminula* is abundant in various water depths from infralittoral to epibathyal in the Mediterranean Sea (Sgarrella and Moncharmont-Zei, 1993; Meriç et al., 2004). *Massilina*, *Quinqueloculina*, *Miliolinella* and *Rosalina* prefer environments that have salinity of >32‰ (Murray, 1973). At the lower part of the sedimentary sequence (units P6–P7), highly diverse assemblages with dominance of *Elphidium*, *Ammonia* and *Quinqueloculina* reflect a shallow marine environment. *A. parasovica* and *A. tepida* are known to be euryhaline and can tolerate low salinity (1–26‰) conditions in Black Sea sediments (Yanko, 1990; Yanko-Hombach, 2007). Dominance of such an assemblage against other foraminifers and

Marine						Oligohaline				Euryhaline
Loxoconcha rhomboidea	*Loxoconcha stellifera*	*Xestoleberis comunis*	*Xestoleberis dispar*	*Henryhowella asperrima*	*Leptocythere* sp.	*Candona neglecta*	*Heterocypris salina*	*Euxinocythere* sp.	*Ilyocypris gibba*	*Cyprideis torosa*
K1/cm										
							*			*
	*		*		*					*
*	*									
	*									
*	*					*				
*			*							
*			*							*
*			*							*
*		*	*						*	*
*			*							*
*						*				*
*			*		*					*
*		*	*		*					*
*	*		*							*
*			*							*
*			*			*				*
*	*		*							*
*			*							*
*			*				*			*
*			*				*			*
*			*	*						*
*			*	*	*	*				*
*					*					*
*			*		*					*
*			*		*					*
*			*			*				*
*		*	*				*			*
*		*			*	*				*
*			*							*
*			*		*	*			*	*
*			*				*		*	*
*								*		*
*			*				*			*
*								*		*
					*			*		*
*			*			*		*		*
*								*		*
*										*
*			*							*
*			*							*
*			*			*				*
*										*
*								*		*
*		*	*							
*			*							*
*			*							*
GJ/cm										
						*			*	
							*		*	
									*	

decreasing population and poor diversity at the upper unit (P2) indicate a relative decrease in salinity.

Benthic foraminiferal fauna and their vertical distribution pattern in the study area, in general, suggest a transition from shallow marine to brackish water (fluvial–deltaic) conditions in time.

Ostracod fauna (Table 3) consists of 17 marine species (*Aurila convexa*, *Paracytheridea depressa*, *Urocythereis oblonga*, *Pontocythere elongate*, *Semicytherura inverse*, *Semicytherura sulcata*, *Callistocythere intricatoides*, *Carinocythereis carinata*, *Hiltermannicythere turbida*, *Pseudocytherura calcarata*, *Loxoconcha elliptica*, *L. rhomboidea*, *L. stellifera*, *Xestoleberis comunis*, *X. dispar*, *Henryhowella asperrima*, and *Leptocythere* sp.) and 4 oligohaline species (*Candona neglecta*, *Heterocypris salina*, *Euxinocythere* sp., and *Ilyocypris gibba*) and 1 euryhaline species (*Cyprideis torosa*). *Aurila*, *Semicytherura*, *Urocythereis*, *Callistocythere*, *Pseudocytherura*, and *Pontocythere* from marine ostracod genera are common in sandy units of location K1. A few marine species (4–5 species) are found in unit P7 (below 831 cm). Low population and diversity both start to increase in unit P6, reaching their maximum abundance (10–12 species) between 576- and 756-cm intervals in units P5 and P4. This indicates that the salinity change towards marine condition in the environment. Oligohaline ostracods (*C. neglecta*, *H. salina*, and *I. gibba*) are found in all the units of the sequence together with marine ostracods, suggesting some sporadic fresh–brackish water input. Presence of only oligohaline ostracods in the black clay swamp deposit below the sequence (location GJ) indicates that they were deposited under freshwater conditions (Table 3).

Archeological evidence

As noted above, units P5, P4, P3 and P2 include extensive findings from Byzantine times up to the Ottoman period, the well-preserved remains of 34 Byzantine ships being the most spectacular of them. In the gravel clusters underlying the marine sediments, a few conspicuous sherds that are characteristic of the Early Iron Age, (~1100–85 BC, Özdoğan, 2003) have been recovered. The most exclusive prehistoric material from unit P7 in and amongst the gravel-cobble layer can be grouped under the following headings:

a) *In situ material among the gravel-cobble*: above the Miocene-aged basement, a dense accumulation of cobble-sided stones were recovered; evidently most of them had sunk from upper horizons when the subsequent cultural layers were eroded during the transgression of the SOM. However, it was still possible to trace architectural features such as stone alignments and post-holes on the surface of the basement. The archeological material recovered within this fill consists of pottery sherds, animal bones, flint tools or debris, almost all of them characteristic of the archaic stage of the Fikirtepe Culture (~6600 BC; Özdoğan, 2008).
b) *Burials*: a number of human burials have been recovered, some from the areas adjacent to the gravel-cobble, and others cut into the black clay of the swamp deposit. As it is customary to place burials in deeply dug pits, it is possible to surmise that they are later than the earliest occupation layer. Two of the burials were simple inhumations where the dead were placed on a wooden plank in a tightly flexed position. A number of burial gifts were also recovered. The pottery vessels that are found in association with the burials display advanced features of the Fikirtepe culture, more akin to the so-called Yarımburgaz 4 culture, dated to 5530–5570 BC (Özdoğan, 2003). On the other hand, in pits cut into the surface of the clayey deposit nine cremation burials were recovered, six of them in burial jars, the others in cremation pits. It is of interest to note that the archeological material recovered with the cremations also points to the later stages of the Fikirtepe–Yarımburgaz 4 culture.
c) *Mixed archeological material found on and in the gravel-cobble*: numerous archeological materials, sherds, lithics, and bones have been collected. The sherds present a rather wide cultural spectrum, Archaic Fikirtepe being the earliest and Toptepe type material the youngest. However, dominant among the material are the sherds showing typical features of the Yarımburgaz 4 and 3/2 cultures. It is evident that none of them are *in situ* and that all of them are of secondary deposition.

A wide range of archeological material was also collected from the black clay swamp deposit. Along with conventional material such as sherds, lithic fragments, and faunal remains were numerous wooden implements, tree trunks and well preserved plant and cereal remains—all worth noting, as on other land sites they are not preserved.

Discussion

Changing sea level and sedimentary environments from ~9 cal ka BP to present

The transgressive and progradational sedimentary sequences at the Yenikapı excavation site indicate a rising sea level on land, followed by a coastal progradation during the Holocene highstand. Above the Miocene basement and swamp deposit, the base of unit P7 reflects the beginning of the transgression and/or Maximum Flooding Surface (MFS) at −6 m below the present sea level (Fig. 5). Coarse sandy shell hash facies intercalated with small gravels and pebbles were interpreted to be the reworked sediments from the shore which was further to the south. Large gravels and cobbles should have been mostly derived from the shelf area of the SOM, which was subaerially exposed during the glacial periods. Gravels derived from Paleozoic age formations which do not exist in the drainage area of Lykos Stream (Fig. 3) were probably brought by the Bosporus (when it was a river during glacial periods) and spread out onto the shelf area close to Yenikapı. At about 8–9 cal ka BP, the sea level must have been much lower than 6 m, probably −15 m lower than the present level, considering the results of Perissoratis and Conispoliatis (2003), Lambeck and Bard (2000), Lambeck et al. (2004). Lykos stream was evidently discharging to the SOM farther to the south of the present coastline (Fig. 9a). Radiocarbon ages from the base of unit P7 (just above the swamp) indicate that the marine transgression of the land had occurred around ~6.8–7 cal ka BP (Fig. 9b), drowning the stream. The drowning of littoral areas (such as lagoons and deltas) to the NE of the SOM and along the Bosporus coast by the rising sea level at about 7 cal ka BP was shown with the changing benthic fauna from the long boreholes (Meriç and Algan, 2007). The maximum sea level rise reaching the upper course of Lykos Stream created an inlet (Fig. 9b), which must have provided, later, a natural shelter for the use of local cultures from probably the Early Bronze Age to Byzantine times.

Ages consistent with ~3 cal ka BP within and from the upper boundary of P7 (Fig. 5) might be condensed due to sediment starvation as the marine incursion pushed the inflows of Lykos Stream inland in conjunction with the base level rise (Nichols, 1999; Coe and Church, 2003). Sediment inputs became sufficient to be deposited only after ~3 cal ka BP (Fig. 9c). Dredging during Roman times is known to have created hiatuses by removing the oldest material in ancient harbors, such as the absence of strata between 4000 and 500 BC in Tyre (Marriner and Morhange, 2006a, 2007). However, within unit P7 no discontinuity or scour from such an activity was observed; besides, the time interval for this absence corresponds to ~5000 and 1000 BC, much earlier than the establishment of the Byzantine Harbor.

Unit P6 with its current/wave rippled sands represents the lower/middle shoreface sediments. Although the origin of the chaotic layer is not certain yet, fining grain size, heterometric granulometry, and anthropogenic content of P5 reflects the ancient harbor sediments (*sensu* Marriner and Morhange, 2006b, 2007). Deposition of these fine grained sediments could have been instigated by new harbor

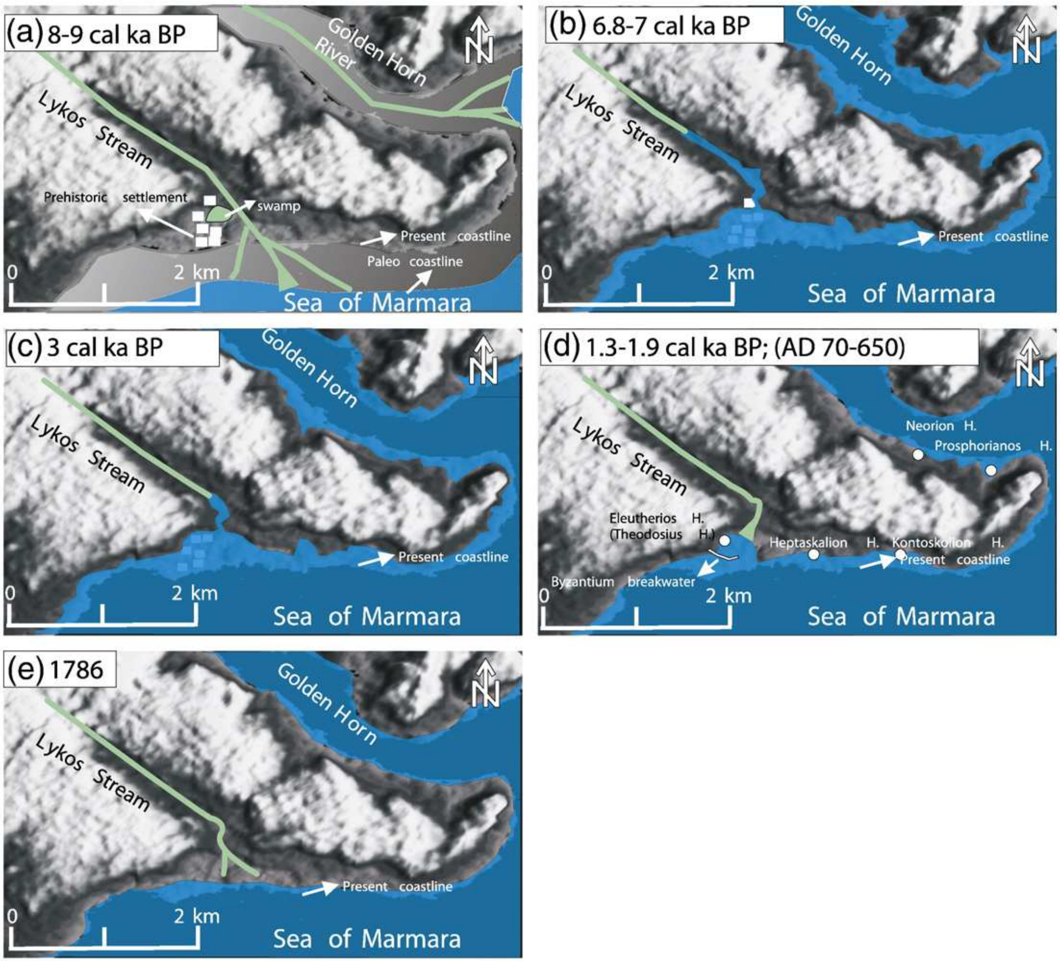

Figure 9. Reconstruction of the coastal environment during the Holocene. (a) ~8–9 cal ka BP; the paleocoastline was further to the south. (b) ~6.8–7 cal ka BP; inundation of Lykos Stream to its upper course. (c) ~3 cal ka BP; coastal progradation started (d) ~1.3–1.9 cal ka BP; (AD 70–650); Theodosian and other harbors during the Byzantine period. (e) 18th century; approximate position of the coastline at 1786 (from a historical map produced by Kauffer and J. B. Le Chevalier, in Kubilay, 2010). The base map is produced from Fig. 2. Shading of the relief is lighter to darker from high altitude to low.

infrastructures, such as a breakwater, which would have produced a protected small basin with low-energy conditions. Therefore, the transition from the medium sands of unit P6 to silts and clays of unit P5 denotes the beginning of a confined harbor basin (Marriner and Morhange, 2006b, 2007; Marriner et al., 2010). Dates within unit P5 from locations K1 and K3 are around ~1.3–1.9 cal ka BP (~AD 70–650), covering the time for the founding of the harbor by Emperor Constantine I or Theodosius I (Fig. 9d). Relatively well-sorted medium to fine sands of units P4 and P3 are upper shoreface sediments, indicating intensive coastal progradation. This reconversion to natural high-energy conditions was probably related to the increase of sediment input, as well as human activities (agriculture) along Lykos Stream and in the city, increasing erosion on land, as observed in other ancient harbors of the eastern Mediterranean (Marriner and Morhange, 2007). Finally, P2 represents the fluvial–deltaic sediments deposited from Lykos Stream, below the artificial fillings of P1. The coastline close to that of the present one must have formed before the 18th century. In the first map of İstanbul scientifically drawn with measuring instruments by F. Kauffer and J. B. Le Chevalier (J. B. Le Chevalier, *Voyage de la Propontide et du Pont-Euxin*; from Kubilay, 2010), the coastline in 1786 was shown to be straight, as in Figure 9e.

Archeological perspective (impacts on cultural environment)

There are as yet no absolute dates available from the prehistoric layers; however, large amounts of diagnostic pottery sherds have been recovered which display the distinct features of various cultural assemblages previously recorded and dated from other excavations in northwestern Turkey. What is significant is the rather large time-span represented in this fill; among the typologically datable sherds, the latest are of the so-called "Toptepe Culture" (Parzinger and Schwarzberg, 2005), contemporary with middle Karanovo IV of Bulgaria and Aşağı Pınar 3-2 of Eastern Thrace (5730–5540 BC; CANEW, 2006). Even though material of this stage is rather slight, nevertheless the presence of diagnostic sherds makes this affiliation secure. On the other hand, the material found in this horizon was mostly of Archaic Fikirtepe, Classical Fikirtepe, Yarımburgaz 4 and 3/2 horizons, covering the time range between 6600 and 5530 BC. There were also a few, but rather dubious, sherds that might be of an earlier age. In an overall assessment it is clear that the Neolithic settlement lasted for a considerable duration, almost a millennium before being inundated by the rising level of the sea.

Even though *in situ* remains of architecture are extremely fragmentary, the dwellings must have been simple huts, round or oval in plan and built in the so-called wattle and daub technique with some stone reinforcements. Other sites of the Fikirtepe culture in the environments of İstanbul, such as the type-site of Fikirtepe and Pendik have revealed similar structures (Özdoğan 1999). The settlement, like in most other settlements of its time, seems to have been encircled by a palisade-like construction that has been preserved as an alignment of cobble and gravel clusters. Due to the state of preservation of the remains, it is not possible to define the extent of the settlement; however, it seems to be at least as big as the Neolithic settlement at

Pendik which was about 300 × 200 m in size. The material assemblage, the pottery, the lithic finds, as well as the bone industry, consists mainly of the known types from other excavations; thus the settlement at Yenikapı accords well with the previously attested cultures in the region. On the other hand, the presence of cremated burials is unique to the site; previously no cremated burials of the Neolithic period had been recovered in Anatolia and there are only a few odd cases reported from Greece and Bulgaria. Even though it is still too early to remark on their presence at Yenikapı, the fact that both inhumated and cremated burials had similar associated archeological finds shows that communities with different belief systems were living together at the site. Whether this represents the merging of local Mesolithic communities with migrant farmers from inner Anatolia will be clear only after the results of the DNA analysis are complete.

The location of the Neolithic settlement at Yenikapı is similar to other contemporary sites, being located within easy reach of the sea coast, some hundreds of meters inland by a stream and a small swamp. As in all other contemporary sites, marine sources—both open-sea fishing and mollusk collecting—played a critical role in subsistence. What happened following the marine invasion of the area is not clear; however, it is possible to surmise that the inhabitants may have moved further inland, along Lykos Stream, though there is yet no evidence of any 4th to 2nd millennium habitation from the immediate vicinity. The presence at Yenikapı of a few Early Iron Age sherds datable to the very beginning of the 1st millennium BC, presents a problem. At present we surmise that they must have originated from a nearby settlement; at least one Early Iron Age settlement had previously been located in İstanbul (Fıratlı, 1973).

Conclusion

Archeological excavation in the ancient harbor of İstanbul at Yenikapı has revealed a sequence deposited during the Holocene highstand. The pre-Holocene surface is mainly composed of Miocene bedrock and locally of swamp deposits. Ships and numerous objects of the Byzantine period and various remnants of a Neolithic settlement, including burial places, were found within and below the sedimentary sequence. The presence and altitude of a Neolithic settlement in the region clearly indicates that the sea level was lower than −6 m than that of the present, at about 8–9 cal ka BP. In this respect, it is worth noting that during the initial stage of the Fikirtepe culture which is the Archaic Phase, the level of the SOM must have been 15 to 20 m lower than present, and hence there must have been extensive coastal plains that are now submerged. This condition must have been persistent as the lifespan of the Yenikapi continued up to the Toptepe cultural stage. A maximum marine ingression occurring at 6.8–7 cal ka BP formed an inlet at the mouth of Lykos Stream. Coastal progradation became evident after ~3 cal ka BP in this natural harbor. Transition from sand to fine-grained sediments indicates the construction of the Byzantine Harbor. The sedimentation rate was accelerated due to coastal progradation and anthropogenic factors (harbor and urban activities) during deposition of units P5, P4, and P3.

Acknowledgments

We are grateful to Directors Dr. İsmail Karamut, Zeynep Kızıltan, chief archeologists Metin Gökçay and Yaşar Anılır, and site archeologist Sırrı Çömlekçi for their valuable and kind help at the field study. We thank Dr. Baki Yokeş for identifying mollusk samples for radiocarbon analysis. We are indebted to Prof. Peter Kuniholm and Dr. Charlotte Pearson for improving the English language of the manuscript. We acknowledge two anonymous reviewers and Senior Editor Dr. D. B. Booth for their constructive comments on the earlier version of the manuscript. The present work was supported by the Research Fund of İstanbul University, project number ÖNAP-472.

References

Aksu, A.E., Hiscott, R.N., Yaşar, D., 1999. Oscillating Quaternary water levels of the Marmara Sea and vigorous outflow into the Aegean Sea from the Marmara Sea–Black Sea drainage corridor. Marine Geology 153, 275–302.

Aksu, A.E., Hiscott, R.N., Kaminski, M.A., Mudie, P.J., Gillespie, H., Abrajano, T., Yaşar, D., 2002. Last glacial–Holocene paleoceanography of the Black Sea and Marmara Sea: stable isotopic, foraminiferal and coccolith evidence. Marine Geology 190, 119–149.

Algan, O., Yalçın, M.N., Yılmaz, Y., Perinçek, D., Özdoğan, M., Yılmaz, İ., Meriç, E., Sarı, E., Kırcı-Elmas, E., Ongan, D., Bulkan-Yeşiladalı, Ö., Danışman, G., Özbal, H., 2007. Antik Theodosius Yenikapı Limanının Jeoarkeolojik Önemi: Geç-Holosen ortam değişimleri ve İstanbul'un son 10 000 yıllık kültürel tarihi. In: Kızıltan, Y. (Ed.), Gün Işığında İstanbul'un 8000 Yılı, Marmaray, Metro, Sultanahmet kazıları: Vehbi Koç Vakfı–İstanbul Arkeoloji Müzeleri, İstanbul, pp. 242–245. In Turkish.

Algan, O., Yalçın, M.N., Özdoğan, M., Yılmaz, İ., Sarı, E., Kırcı-Elmas, E., Ongan, D., Bulkan-Yeşiladalı, Ö., Yılmaz, Y., Karamut, İ., 2009. A short note on the geo-archaeological significance of the ancient Theodosius Harbor (İstanbul—Turkey). Quaternary Research 72, 457–461.

Algan, O., Yalçın, M.N., Yılmaz, İ., Kırcı-Elmas, E., Sarı, E., Ongan, D., Bulkan-Yeşiladalı, Ö., Perinçek, D., Özdoğan, M., Yılmaz, Y., Karamut, İ., 2010. Geoarchaeology of the Theodosian Harbor at Yenikapı. In: Kocabaş, U. (Ed.), Proceedings of the 1st Symposium on Marmaray–Metro Salvage Excavations 5th–6th May 2008. İstanbul Arkeoloji Müzeleri Müdürlüğü, pp. 175–181.

Breman, E., 1975. The Distribution of Ostracodes in the Bottom Sediments of the Adriatic Sea. Vrije Universiteit te Amsterdam, Krips Repro, Meppel, p. 165.

Brückner, H., Müllenhoff, M., Handl, M., van der Borg, K., 2002. Holocene landscape evolution of the Büyük Menderes alluvial plain in the environs of Myous and Priene (Western Anatolia Turkey). Zeitschrift für Geomorphologie, Supplement Band 127, 47–65.

Çağatay, M.N., Görür, N., Algan, O., Eastoe, C., Tchapalyga, A., Ongan, D., Kuhn, T., Kuşcu, İ., 2000. Last glacial–Holocene palaeoceanography of the Sea of Marmara: timing of the last connections with the Mediterranean and the Black Sea. Marine Geology 167, 191–206.

Çağatay, M.N., Görür, N., Polonia, A., Demirbağ, E., Sakınç, M., Cormier, M.-H., Capotondi, L., McHugh, C., Emre, Ö., Eriş, K., 2003. Sealevel changes and depositional environments in the İzmit Gulf, eastern Marmara Sea, during the late glacial–Holocene period. Marine Geology 202, 159–173.

CANEW, 2006. CANeW Aegean Catchment ^{14}C Chart by Thissen, L. http://canew.org.

Coe, A.L., Church, K.D., 2003. Sequence stratigraphy and sea-level change (part 2). In: Coe, A.L. (Ed.), The Sedimentary Record of Sea-Level Change. Cambridge University Press, The Open University, pp. 57–98.

Fıratlı, N., 1973. The first settlement of Byzantion. Türkiye Turing ve Otomobil Kurumu Bülteni 38 (317), 21–25.

Flerit, F., Armijo, R., King, G.C.P., Meyer, B., Barka, A., 2003. Slip partitioning in the Sea of Marmara pull-apart determined from GPS velocity vectors. Geophysical Journal International 154, 1–7.

Folk, R.L., Ward, W.C., 1957. Brazos river bar: a study of significance of grain size parameters. Journal of Sedimentary Petrology 27, 3–26.

Galili, E., Zviely, D., Weinstein-Evron, M., 2005. Holocene sea-level changes and landscape evolution on the northern Carmel coast (Israel). Mediterranean 1 (2), 79–86.

Goiran, J.P., Tronchere, H., Salomon, F., Carbonel, P., Djerbi, H., Ognard, C., 2010. Palaeoenvironmental reconstruction of the ancient harbors of Rome: Claudius and Trajan's marine harbors on the Tiber delta. Quaternary International 216 (1–2), 3–13.

Guillaume, M.C., Peypouquet, J.P., Tetart, J., 1985. Quaternaire et actuel. Atlas des Ostracodes de France. In: Oertli, H.J. (Ed.), Bull. Centres Rech. Explor. Prod. Elf-Aquitaine: Mém., 9, pp. 337–377.

Hiscott, R.N., Aksu, A.E., 2002. Late Quaternary history of the Marmara Sea and Black Sea from high-resolution seismic and gravity-core studies. Marine Geology 190, 261–282.

Hiscott, R.N., Aksu, A.E., Mudie, P.J., Marret, F., Abrajano, T., Kaminski, M., Evans, J., Çakıroğlu, A.I., Yaşar, D., 2007. A gradual drowning of the southwestern Black Sea shelf: evidence for a progressive rather than abrupt Holocene reconnection with the eastern Mediterranean Sea through the Marmara Sea Gateway. Quaternary International 167–168, 19–34.

İBB, 2006. İstanbul il alanının genel jeoloji özellikleri. İstanbul Büyükşehir Belediyesi raporu, 1/125.000 ölçekli İstanbul ilinin jeoloji Haritası. http://www.ibb.gov.tr/tr-TR/SubSites/IstanbulVeDeprem/Calismalarimiz/KentJeolojisi/Pages/IstanbulunJeolojikYapisi.aspx.

Jorissen, F.J., 1988. Benthic foraminifera from the Adriatic Sea, principles of phenotypic variation. Ultrecht Micropaleontology Bulletin 37, 1–74.

Karamut, İ., 2007. İstanbul Arkeoloji Müzeleri Müdürlüğü'nce yürütülen kazılar. In: Kızıltan, Y. (Ed.), Gün Işığında İstanbul'un 8000 Yılı. Marmaray, Metro ve Sultanahmet Kazıları. Vehbi Koç Vakfı — İstanbul Arkeoloji Müzeleri, İstanbul, pp. 10–17. In Turkish.

Kocabaş, U., 2010. Istanbul University Yenikapı shipwrecks project: ships. In: Kocabaş, U. (Ed.), Proceedings of the 1st Symposium on Marmaray-Metro Salvage Excavations 5th–6th May 2008. İstanbul Arkeoloji Müzeleri Müdürlüğü, pp. 23–35.

Kraft, J.C., Rapp, G.R., Kayan, I., Luce, J.V., 2003. Harbor areas at ancient Troy: sedimentology and geomorphology complement Homer's Iliad. Geology 31, 163–166.

Kubilay, A.Y., 2010. Maps of Istanbul 1422–1922. Kaptan Yayıncılık Ltd Şti. Denizler Kitapevi. İstanbul, Turkey, p. 255.

Lambeck, K., Bard, E., 2000. Sea-level change along the French Mediterranean coast since the time of the Last Glacial Maximum. Earth and Planetary Science Letters 175 (3–4), 202–222.

Lambeck, K., Antonioli, F., Purcell, A., Silenzi, S., 2004. Sea-level change along the Italian coast for the past 10,000 yr. Quaternary Science Reviews 23, 1567–1598.
Lericolais, G., Popescu, I., Guichard, F., Popescu, S.M., 2007. A Black Sea lowstand at 8500 yr B.P. indicated by a relict coastal dune system at a depth of 90 m below sea level. GSA Special paper 426, 171–188.
Lichter, C., 2004. How did farming reach Europe? Anatolian–European relations from the second half of the 7th through the first half of the 6th millennium cal BC. Byzas 2. Ege Yayincılık, Istanbul.
Major, C.O., Goldstein, S.L., Ryan, W.B.F., Lericolais, G., Piotrowski, A.M., Hajdas, I., 2006. The co-evolution of Black Sea level and composition through the last deglaciation and its paleoclimatic significance. Quaternary Science Reviews 25, 2031–2047.
MARMARAY Tube Tunnel Project, 2005. Final Geotechnical Factual Report. Taisei Corporation, STFA Temel Araştırma ve Sondaj A.Ş.
Marriner, N., Morhange, C., Boudagher-Fadel, M., Bourcier, M., Carbonel, P., 2005. Geoarchaeology of Tyre's ancient northern harbor, Phoenicia. Journal of Archaeological Science 32, 1302–1327.
Marriner, N., Morhange, C., 2006a. Geoarchaeological evidence for dredging in Tyre's ancient harbor, Levant. Quaternary Research 65, 164–171.
Marriner, N., Morhange, C., 2006b. The 'Ancient Harbor Parasequence': anthropogenic forcing of the stratigraphic highstand record. Sedimentary Geology 186, 13–17.
Marriner, N., Morhange, C., 2007. Geoscience of ancient Mediterranean harbors. Earth-Science Reviews 80, 137–194.
Marriner, N., Morhange, C., Carayon, N., 2008. Ancient Tyre and its harbors: 5000 years of human–environment interactions. Journal of Archaeological Science 35, 1281–1310.
Marriner, N., Morhange, C., Goiran, J.P., 2010. Coastal and ancient harbor geoarchaeology. Geology Today 26 (1), 21–27.
Meisch, C., 2000. Freshwater Ostracoda of Western and Central Europe. Süßwasserfauna von Mitteleuropa 8/3. Spektrum, Heidelberg.
Meriç, E., Yanko, V., Avşar, N., Meriç, E., Yanko, V., Avşar, N., 1995. İzmit Körfezi (Hersek Burnu–Kaba Burun) Kuvaterner istifinin foraminifer faunası. (Foraminiferal fauna of the Quaternary sequence in the Gulf of İzmit (Hersek Burnu–Karaburun). In: Meriç, E. (Ed.), İzmit Körfezi Kuvaterner İstifi (Quaternary Sequence in the Gulf of İzmit), Kocaeli Valiliği Çevre Koruma Vakfı. ISBN: 975-96123-0-5, pp. 105–153. In Turkish.
Meriç, E., Avşar, N., Bergin, F., 2004. Benthic foraminifera of eastern Eagean Sea (Turkey) systematics and autoecology. Turkish Marine Research Foundation, İstanbul, 18, p. 306.
Meriç, E., Algan, O., 2007. Paleoenvironments of the Marmara Sea (Turkey) coasts from paleontological and sedimentological data. Quaternary International 167–168, 128–148.
Morhange, C., Goiran, J.-P., Bourcier, M., Carbonel, P., Le Campion, J., Rouchy, J.-M., Yon, M., 2000. Recent Holocene paleoenvironmental evolution and coastline changes of Kition, Larnaca, Cyprus, Mediterranean Sea. Marine Geology 26, 205–230.
Morhange, C., Laborel, J., Hesnard, A., 2001. Changes of relative sea level during the past 5000 years in the ancient harbor of Marseilles, Southern France. Palaeogeography, Palaeoclimatology, Palaeoecology 166, 319–329.
Morhange, C., Blanc, F., Schmitt-Mercury, S., Bourcier, M., Carbonel, P., Oberlin, C., Prone, A., Vivent, D., Hesnard, A., 2003. Stratigraphy of late-Holocene deposits of the ancient harbor of Marseilles, southern France. The Holocene 13 (2), 323–334.
Müller-Wiener, W., 2001. İstanbul'un Tarihsel Topoğrafyası. Yapı Kredi Yayınları, 1419, p. 534. In Turkish.
Murray, J.W., 1973. Distribution and Ecology of Living Benthic Foraminiferids. Crane Russak and Co, New York, p. 274.
MTA (General Directorate of Mineral Research and Exploration), 2002. 1:100 000 ölçekli açınsama nitelikli Türkiye Jeoloji Haritaları, No: 65, İstanbul F21 paftası. Jeoloji Etütleri Dairesi, Ankara.
Nichols, G., 1999. Sedimentology and Stratigraphy. Blackwell Science Ltd, p. 355.
Özdoğan, M., 1997. Anatolia from the Last Glacial Maximum to the Holocene Climatic Optimum: cultural transformations and the impact of the environmental setting. Paléorient 23 (2), 24–38.
Özdoğan, M., 1999. Northwestern Turkey: Neolithic cultures in between the Balkans and Anatolia. In: Özdoğan, M. (Ed.), Neolithic in Turkey, Arkeoloji ve Sanat yayınları, pp. 203–224.
Özdoğan, M., 2003. The Black Sea, the Sea of Marmara and Bronze Age archaeology—an archaeological predicament. In: Wagner, G., Pernicka, E., Uerpmann, H.P. (Eds.), Troia and the Troad. Springer, Berlin, pp. 105–120.
Özdoğan, M., 2006. Neolithic cultures at the contact zone between Anatolia and the Balkans—diversity and homogeneity at the Neolithic frontier. In: Gatsov, I., Schwarzberg, H. (Eds.), Aegean–Marmara–Black Sea: The Present State of Research on the Early Neolithic. Langenweissbach, pp. 21–28.
Özdoğan, M., 2007. Marmara Bölgesi Neolitik Çağ Kültürleri. In: Özdoğan, M., Başgelen, N. (Eds.), Anadolu'da Uygarlığın Doğuşu ve Avrupa'ya Yayılımı. Türkiye'de Neolitik Dönem: Yeni Kazılar, Yeni Bulgular, Arkeoloji ve Sanat Yayınları, İstanbul. pp. 401–426 (text), 405–430 (Plates). (In Turkish).
Özdoğan, M., 2008. An alternative approach in tracing changes in demographic composition: the westward expansion of the Neolithic way of life. In: Bocquet-Appel, J., Bar Yosef, O. (Eds.), The Neolithic Demographic Transition and Its Consequences. Springer, Heidelberg, pp. 139–178.
Parzinger, H., Schwarzberg, H., 2005. Aşağı Pınar II. Die mittel- und spätneolithische Keramik. Verlag. Philipp von Zabern, Mainz.
Perinçek, D., Meriç, E., Pulak, C., Körpe, R., Yalçıner, A.C., Gökçay, M., Avşar, N., Nazik, A., Kozanlı, C., Kapan Yeşilyurt, S., Gökgöz, Z., 2007. Yenikapı Antik Liman Kazılarında Jeoarkeoloji Çalışmaları ve Yeni Bulgular. Türkiye Jeoloji Kurultayı, 60, pp. 16–22. Nisan 2007, Ankara. (In Turkish).
Perinçek, D., 2010. Geoarchaeology of the excavation site for the last 8000 years and traces of natural catastrophes in the geological profile. In: Kocabaş, U. (Ed.), Proceedings of the 1st Symposium on Marmaray-Metro Salvage Excavations 5th–6th May 2008. İstanbul Arkeoloji Müzeleri Müdürlüğü, pp. 191–219.
Perissoratis, C., Conispoliatis, N., 2003. The impacts of sea-level changes during latest Pleistocene and Holocene times on the morphology of the Ionian and Aegean seas (SE Alpine Europe). Marine Geology 196, 145–156.
Pinhasi, R., 2003. A new model for the spread of the first farmers in Europe. Documenta Praehistorica XXX 1–47.
Pondard, N., Armijo, R., King, G.C.P., Meyer, B., Flerit, F., 2007. Fault interactions in the Sea of Marmara pull-apart (North Anatolian Fault): earthquake clustering and propagating earthquake sequences. Geophysical Journal International 171, 1185–1197.
Pulak, C., 2007. Yenikapı Bizans batıkları. In: Kızıltan, Z. (Ed.), Gün Işığında İstanbul'un 8000 Yılı, Marmaray, Metro, Sultanahmet kazıları, Vehbi Koç Vakfı — İstanbul Arkeoloji Müzeleri, İstanbul, pp. 202–215 (In Turkish).
Reilinger, R.E., Ergintav, S., Bürgmann, R., McClusky, S., Lenk, O., Barka, A., Gürkan, O., Hearn, L., Feigl, K.L., Çakmak, R., Aktuğ, B., Özener, H., Töksoz, M.N., 2000. Coseismic and Postseismic Fault Slip for the 17 August 1999, M = 7.5, Izmit, Turkey Earthquake. Science 289, 1519–1524.
Ryan, W.B.F., Pitmann III, W.C., Major, C.O., Shimkus, K., Moskalenko, V., Jones, G.A., Dimitrov, P., Görür, N., Sakınç, M., Yüce, H., 1997. An abrupt drowning of the Black Sea shelf. Marine Geology 138, 119–126.
Ryan, W.B.F., Major, C.O., Lericolais, G., Goldstein, S.L., 2003. Catastrophic flooding of the Black Sea. Annual Review of Earth and Planetary Sciences 31, 525–554.
Sayar, C., 1977. İstanbul Yeni İskan Yöreleri Geoteknik ve Sismik Etüdü. Boğaziçi Üniversitesi, Deprem Mühendisliği Arastırma Enstitüsü Raporu, Cilt 1. , p. 119 (In Turkish).
Sgarrella, F., Moncharmont-Zei, M., 1993. Benthic foraminifera of the Gulf of Naples (Italy): systematics and autoecology. Bollettino della Societa Paleontologica Italiana 32 (2), 145–264.
Siani, G., Paterne, M., Arnold, M., Bard, E., Métivier, B., Tisnerat, N., Bassinot, F., 2000. Radiocarbon reservoir ages in the Mediterranean Sea and Black Sea. Radiocarbon 42 (2), 271–280.
Sivan, D., Wdowinski, S., Lambeck, K., Galili, E., Raban, A., 2001. Holocene sea-level changes along the Mediterranean coast of Israel, based on archaeological observations and numerical model. Palaeogeography, Palaeoclimatology, Palaeoecology 167, 101–117.
Stanley, D.J., Blanpied, C., 1980. Late Quaternary water exchange between the eastern Mediterranean and the Black Sea. Nature 285, 537–541.
Stanley, D.J., Bernasconi, M.P., 2006. Holocene depositional patterns and evolution in Alexandria's Eastern Harbor, Egypt. Journal of Coastal Research 22, 283–297.
Stuiver, M., Reimer, P.J., Reimer, R., 2005. CALIB RADIOCARBON CALIBRATION PROGRAM. http://calib.qub.ac.uk/calib.
Toksöz, M.N., Reilinger, R.E., Doll, C.G., Barka, A.A., Yalçın, N., 1999. Izmit (Turkey) Earthquake of 17 August 1999: first report. Seismological Research Letters 70 (6), 669–679 November/December 1999.
Van Morkhoven, F.P.C.M., 1963. Post Palaeozoic Ostracoda. Elsevier Amsterdam 2, 478.
Yanko, V., 1990. Stratigraphy and paleogeography of the marine Pleistocene and Holocene deposits of the southern seas of the USSR. Memorie della Societa Geologica Italiana 44, 167–187.
Yanko-Hombach, V.V., 2007. Controversy over Noah's Flood in the Black Sea: geological and foraminiferal evidence from the shelf. In: Yanko-Hombach, V., Gilbert, A., Panin, N., Dolukhanov, P. (Eds.), The Black Sea Flood Question: Changes in Coastline, Climate, and Human Settlement. NATO Science Series IV — Earth and Environmental Sciences, Kluwer Academic Press, Springer, Dordrecht, The Netherlands, pp. 149–205.
Yılmaz, Y., 2007. Morphotectonic development of the southern Black Sea Region and the Bosphorus Channel. In: Yanko-Hombach, V., Gilbert, A., Panin, N., Dolukhanov, P. (Eds.), The Black Sea Flood Question: Changes in Coastline, Climate, and Human Settlement. NATO Science Series IV — Earth and Environmental Sciences. Kluwer Academic Press, Springer, Dordrecht, The Netherlands, pp. 537–569.
Yılmaz, Y., Gökaşan, G., Erbay, A.Y., 2010. Morphotectonic development of the Marmara Region. Tectonophysics 488, 51–70.